UNLV | UNIVERSITY LIBRARIES

12-2011

Energy-based analysis of utility scale hybrid power systems

Kwame Agyenim-Boateng
University of Nevada, Las Vegas

ENERGY-BASED ANALYSIS OF UTILITY SCALE HYBRID POWER SYSTEMS

By

Kwame Agyenim-Boateng

Bachelor of Science
Kwame Nkrumah University of Science and Technology, Ghana
2002

Master of Science
Loughborough University, Britain
2006

A thesis submitted in partial fulfillment
of the requirements for the

Master of Science in Mechanical Engineering

Department of Mechanical Engineering
Howard R. Hughes College of Engineering
The Graduate College

University of Nevada, Las Vegas
December 2011

THE GRADUATE COLLEGE

We recommend the thesis prepared under our supervision by

Kwame Agyenim-Boateng

entitled

Energy-Based Analysis of Utility Scale Hybrid Power Systems

be accepted in partial fulfillment of the requirements for the degree of

Master of Science in Mechanical Engineering
Department of Mechanical Engineering

Robert Boehm, Committee Chair

Yi-Tung Chen, Committee Member

Suresh Sadineni, Committee Member

Yahia Baghzouz, Graduate College Representative

Ronald Smith, Ph. D., Vice President for Research and Graduate Studies
and Dean of the Graduate College

December 2011

ABSTRACT

Energy-Based Analysis of Utility Scale Hybrid Power Systems

by

Kwame Agyenim-Boateng

Dr. Robert F. Boehm, Examination Committee Chair

Professor of Mechanical Engineering

University of Nevada, Las Vegas

The promise of large-scale use of renewables such as wind and solar for supplying electrical power is tempered by the sources' transient behavior and the impact this would have on the operation of the grid. Among the methods cited for addressing some of those concerns are exploring the complementary nature of solar and wind power generation, and through the use of supplemental energy storage. While the technology for the latter has not been proven to be economical on a large scale at the present time, some assessments of what magnitude is required can be made. An energy–based analysis of utility scale hybrid electric power systems based on wind, solar photovoltaic (PV), energy storage and conventional plants has been performed. The main objective was to optimally size the required energy storage capacities for the given load profile with imposed grid supply generations from wind, solar PV and limited conventional plants outputs. A second objective was to address the question of optimal mix between solar and wind for a considered hypothetical case of 100% renewable energy based grid. The study was

carried out using a Southwestern U.S. utility grid hourly load data of 2008. NREL's Solar Advisor Model (SAM 2010) with TMY3 solar data was used to estimate the solar PV system power generation whereas the wind power output data was obtained from NREL/3TIER Group modeled wind data set developed for the U.S. Western Wind and Solar Integration Studies. It was found for the study area that the diurnal and seasonal output profiles of solar PV and wind power do not have the desired complementary nature for exploitation, with a significant weighting (95%/5%) in favor of solar PV when deployed in tandem. The required energy storage capacity was observed to be highly influenced by the flexibility (or base loading) of the grid system.

ACKNOWLEDGMENTS

I wish to express my heartfelt gratitude to Dr. Robert F. Boehm for providing me with the opportunity to work at the Center for Energy Research (CER) at University of Nevada, Las Vegas. It was a privilege to have him as an academic advisor and course professor. My appreciation goes to the Thesis Advisory Committee for their time and consideration. I would like thank Aaron Sahm and Rick Hurt (both Research Engineers at CER) and Kenneth Stone (with Amonix) for the invaluable support and learning experience while working with them on various projects. Finally, my gratitude goes to my wife and the family for the encouragement throughout the period of this study. It is however noted here that without the favor and mercies of the Sovereign LORD, this piece would not have been realized.

TABLE OF CONTENTS

LIST OF TABLES

LIST OF FIGURES

CHAPTER 1

INTRODUCTION

1.1 Background

Energy remains an essential input to economic development and industrialization of a nation and human life. The world's energy demand has mostly been met by the use of fossil fuels. Studies have predicted that these sources are finite and, moreover, their continuing use has negative environmental and health impacts. In view of this, the management of energy sources, rational utilization of energy, and renewable energy source usage are gaining prominence in energy policy formulation [1].

A screenshot of the United States energy consumption from 2006 to 2010 is presented in Table 1.1 [2]. From Table 1.1, it is observed that except for 2007, renewable energy consumption experienced a steady increase in contrast to the total energy consumption. The worldwide upsurge interest in renewable energy is due to its inexhaustibility (thus, ensuring security of supply) and also, its relative environmental friendly form of electricity generation. Figure 1.1, which is an extract from Table 1.1, shows the renewable energy consumption in the United State's energy supply in 2010. In the period under consideration (i.e. between 2006 and 2010), the renewables share of total consumed energy grew from 6.7% to 8.2%. The nation's renewable energy consumption by energy source from 2006 to 2010 is presented in Figure 1.2. Here, we see that the rise in renewable share was spearheaded by considerable growth in wind energy and some biomass energy additions.

Table 1.1: U.S. energy consumption by energy source, 2006 – 2010 (in quadrillion Btu) [2]

Energy Source	2006	2007	2008	2009	2010
Total	99.624	101.362	99.270	94.485	97.892
Fossil Fuels	84.687	86.251	83.540	78.426	81.338
Coal	22.447	22.749	22.385	19.703	20.707
Coal Coke Net Imports	0.061	0.025	0.040	-0.023	-0.006
Natural Gas[1]	22.224	23.702	23.834	23.343	24.667
Petroleum[2]	39.955	39.774	37.280	35.403	35.970
Electricity Net Imports	0.063	0.106	0.113	0.116	0.064
Nuclear Electric Power	8.215	8.455	8.427	8.356	8.441
Renewable Energy	6.659	6.551	7.191	7.587	8.049
Biomass[3]	3.277	3.503	3.852	3.899	4.295
Biofuels[4]	0.771	0.991	1.372	1.567	1.855
Waste	0.397	0.413	0.436	0.452	0.454
Wood and Derived Fuels	2.109	2.098	2.044	1.881	1.986
Geothermal Energy	0.181	0.186	0.192	0.200	0.212
Hydroelectric Conventional	2.869	2.446	2.512	2.669	2.509
Solar Thermal/PV Energy	0.068	0.076	0.089	0.098	0.109
Wind Energy	0.264	0.341	0.546	0.721	0.924

[1]Includes supplemental gaseous fuels.
[2]Petroleum products supplied, including natural gas plant liquids and crude oil burned as fuel.
[3]Biomass includes: biofuels, waste (landfill gas, MSW biogenic, and other biomass), wood and wood derived fuels.
[4]Biodiesel primarily derived from soybean oil and ethanol primarily derived from corn.
PV = Photovoltaic.
Notes: Data revisions are discussed in the Highlights section.
Totals may not equal sum of components due to independent rounding.
Data for 2010 is preliminary.
Sources: Non-renewable energy: U.S. Energy Information Administration (EIA), Monthly Energy Review (MER) March 2011, DOE/EIA-0035 (2011/03) (Washington, DC, March 2011), Tables 1.3, 1.4a and 1.4b; Renewable Energy: Table 2 of this report.

(Conversion: 1quadrillion = 10^{15} Btu; 1 kWh = 3414 Btu)
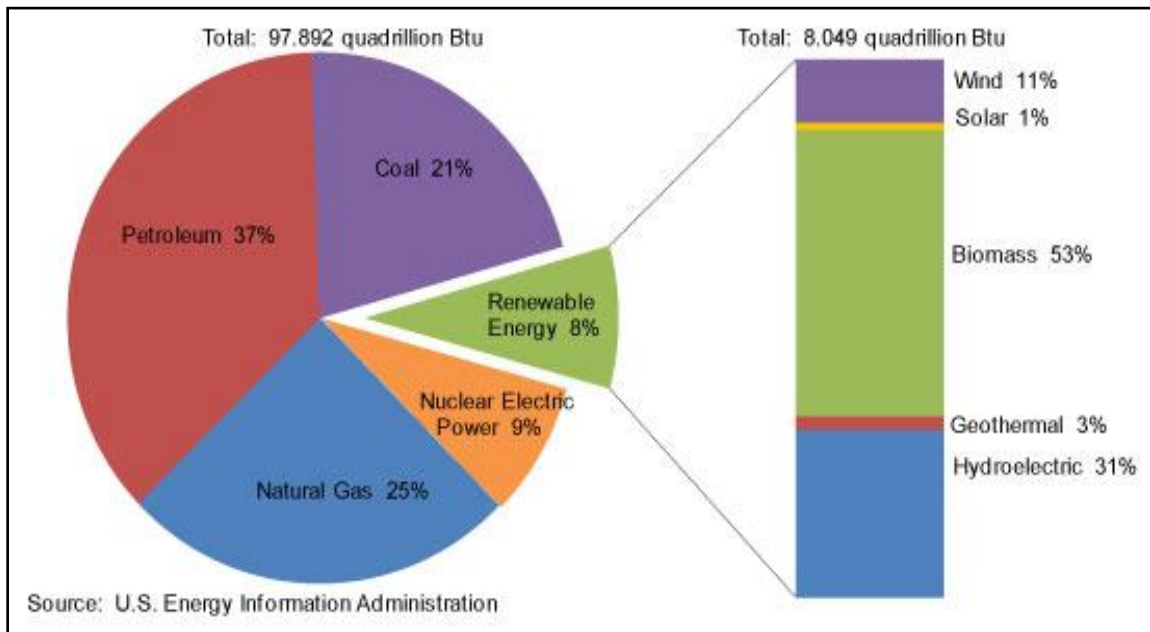
Figure 1.1: Renewable energy consumption in the United Sates energy supply, 2010 [2]
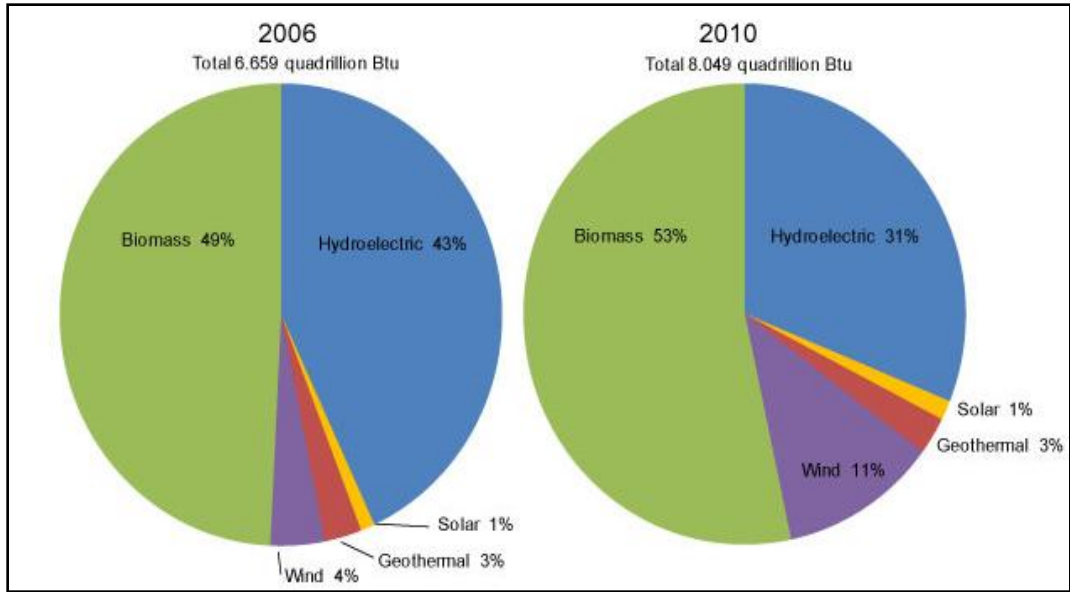
Figure 1.2: U.S. renewable energy consumption by energy source; 2006 and 2010 [2].

The fuel mixes for electricity generation in different regions of the U.S. as of 2009 is presented in Figure 1.3 below.
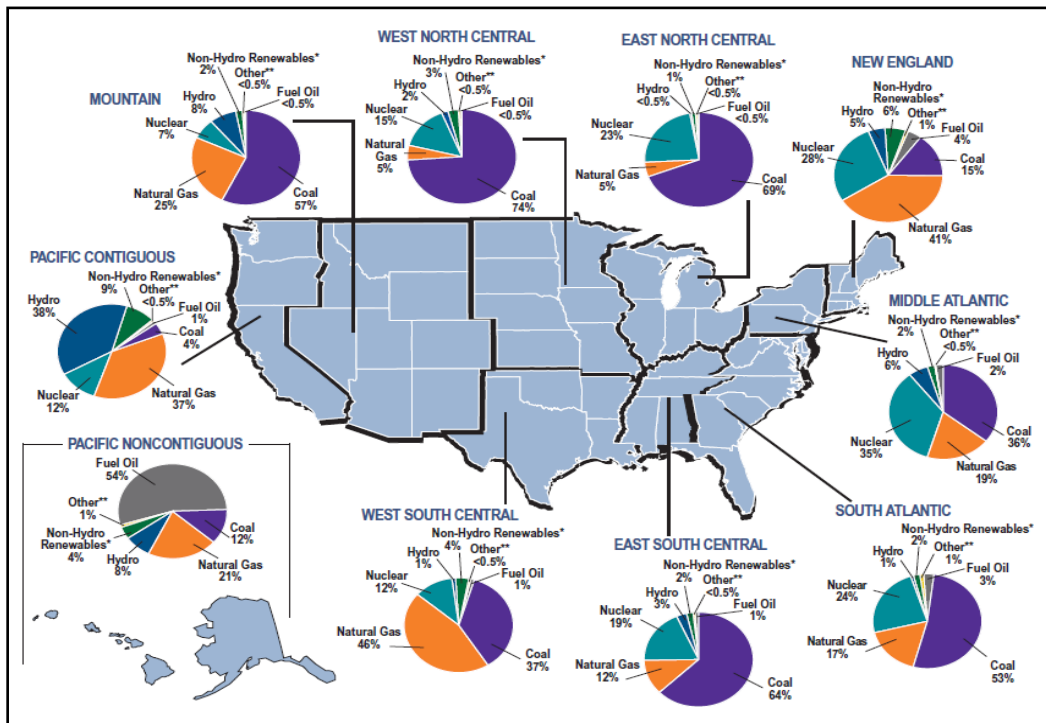
Figure 1.3: U.S regional electricity generation fuel mixes [3]

3

As shown in the Figure 1.3, different regions of the country rely on different fuel mixes which mostly, are influenced by the price and the availability of supply. Fuel diversity holds the key to affordable and reliable electricity by protecting the electric utility companies and consumers from contingencies such as fuel unavailability, price fluctuations, and changes in regulatory practices [3].

According to Nevada Commission on Economic Development [4], renewable energy is the fastest growing industry in the state of Nevada. It also has an aggressive Renewable Energy Portfolio Standard (RPS) that requires all public utilities to generate 25% of their electricity from renewables by 2050, with at least 6% from solar energy through 2016-2025. The state, ranked No. 1 in the United States in solar watts produced per capita, houses some of the world's largest solar installations near Las Vegas:

- 64 MW Parabolic Trough Concentrating Solar Power (3rd largest in the world), with site potential estimate of 2000 MW

- 48 MW Thin-film Photovoltaic Power Generation (largest in North America)

- 14 MW Solar Photovoltaic Power System at Nellis Air Force Base, north of Las Vegas.

Among the potential renewable energy resources in Nevada, wind power is the least exploited for electricity generation. However, the state has wind resources consistent with utility scale production, with good-to-excellent wind resources located in southern Nevada near Las Vegas and near Ely [4].

It is well know that solar power and electricity demand in warmer climates are, in general, positively correlated, and wind power and electricity demand negatively correlated. The solar-demand correlation is mostly associated with air conditioning

demand loads during summer periods. The inherent negative correlation between intermittent solar and wind resources can be exploited as possible complementary power generation options to serve electricity demand in a short-term and/or long-term basis [5].

However, the large-scale deployment of intermittent renewables raises some concerns on the operation of the existing electricity grid which traditionally has been modeled on, and responded very well to, conventional/fossil fuel energy sources of generation. This problem is non-trivial because of the ramping requirements on the grid that already have to meet the fluctuating demand requirements of customers [6,7].

1.2 Study objectives

The state of Nevada is located in the south-western region of the U.S. and has warm climate conditions. As a result of the state's very hot summers, the grid peak loads during this period is quite significant in relation to the other seasons (i.e. winter, spring and fall). In Figure 1.4, the typical summer and winter season's average diurnal grid load profile for southern Nevada is presented.
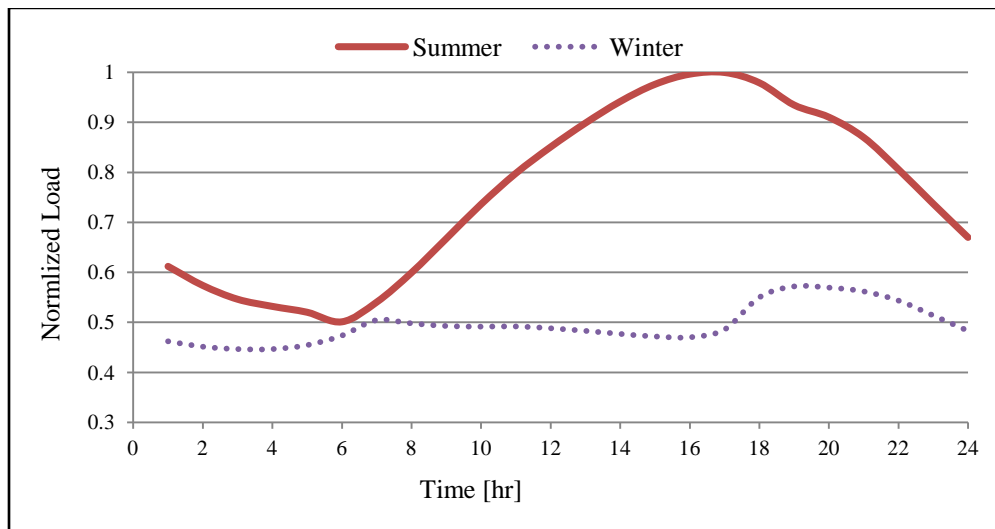
Figure 1.4: Qualitative comparisons of summer and winter average diurnal loads

This presents a major concern to the utility company in the state since to satisfy the enormous summer electricity demand the power company has to commission peaking plants into operation or buy additional power from neighboring states. Both of these options could result in significant increase in operational cost which could put them in financial distress. By extension the customers are also affected due to the differential rate they might have to pay for consumption in that period.

Renewables, especially solar and wind power can compete quite well with the conventional peaking plants in terms of $/kWh cost of delivered electric power. Consequently, the ability to displace the peaking plants which in any case operate for few hours in the year with renewable ('free and inexhaustible' energy input) is seen as laudable. As already mentioned, the inherent intermittency of renewables (such as solar and wind) limits the practicality or success of integrating to the current electric grid structure.

However, several methods exist which can be used to address the intermittency of delivered power of renewable. These include combining geographically disperse intermittent resources of the same type, using supplemental energy storage, and combing different renewables with complementary intermittencies such as wind and solar [8]. In addition to the above methods, other investigators consider methods such as increasing grid flexibility, dumping of surplus renewable energy generation, and load shifting as ways of improving the energy penetration of intermittent renewables [9].

In view of addressing the intermittent output of renewables and shaving of the annual peak grid load (i.e. in summer period), this research study has as its general objective to

examine utility-scale hybrid electric power systems with solar energy, wind energy and electrical energy storage for serving a typical southwestern utility load profile of 2008.

In particular, the maximum required storage capacities for different PV/wind system sizes will be determined. An evaluation of the daily and seasonal peak load shifting by employing varying storage capacities will be carried out. The average energy penetration based on the usable solar PV/wind output will also be examined under these conditions and at different levels of system flexibility. An attempt will be made at evaluating the seasonal optimal mix of solar and wind power for matching the load demand profile.

1.3 Organization of the Thesis

The thesis is organized under five main sections/chapters. In Chapter 1 (Introduction) a brief background is presented on the U.S. energy consumption from 2006 to 2010, as well as the regional resource mixes for electricity generation. Moreover, notable solar installations in the state of Nevada are highlighted and followed by the layout of the objectives of the study.

Chapter 2 (Literature Review) gives an overview of solar energy, wind energy, and storage technologies. A review of published research articles on utility-scale hybrid power systems is covered in this section

In the Chapter 3 (Methodology) the grid load data for the analysis are given. The details of the methods used for accessing the PV energy generation and wind energy generation data are explained in this section. The logic for the algorithms developed in MATLAB for the study analysis is presented.

Chapter 4 (Simulation Results and Discussion) highlights the key results obtained from the model simulations and the accompanying discussions with focus on their significance to the power utility industry.

Finally, in Chapter 5 (Conclusion and Recommendations) the conclusions drawn from the study, the limitations of the project and some recommendations for further works to improving the study are presented.

Further information about the MATLAB modeling can be found in the appendix.

CHAPTER 2

LITERATURE REVIEW

2.1 Overview of solar and wind energy technologies

2.1.1 Solar energy

Solar energy is the energy from the sun, and for which humans have always used as far back as they have existed on this planet. It is also the driving mechanism behind other renewable energy sources such as wind, bioenergy, and hydropower. Outside the earth's atmosphere it has an intensity of more than 1 kW/m^2, however, with an average daily interception of about 4 kWh/m^2 on the earth surface due to attenuation (from absorption and reflection) by the earth's atmosphere. The potential of this energy resource is enormous, and it is estimated that the solar energy intercepted by the earth in less than one month is equivalent of all the energy originally stored in conventional energy resources of coal, petroleum, and natural gas on the planet [10].

The conversion of the solar energy resource to electricity is achieved basically in two ways referred to as direct and indirect. With the direct conversion, which is the method considered in this work, a photovoltaic cell (which is an electrical semiconductor) is adapted where the energy contained in the sun (photons) penetrating the cell is transferred to the electrons. The excited electrons are then channeled into an external circuit generating current for powering an electrical load. For useful electric power output the cells are connected in series (to increase the voltage) and parallel (to increase the current) into modules and arrays. Mostly, inverters are employed to convert the DC

output from the PV modules to AC before integrating it to the electric transmission or distribution grid for consumption.

With the indirect method, thermodynamic processes are employed to convert sunlight into electricity. Here concentrating solar collectors are used to collect and focus the solar radiation, and generating thermal energy which is then transferred to a steam boiler as the source of heat input. Power cycles such as Rankine, Brayton, or Stirling are used to convert the thermal energy to work by driving a turbine connected to an electric generator. The solar collectors used are of three main designs: parabolic troughs and dishes, non-imaging concentrators, and central receivers.

2.1.2   Wind energy

Wind energy involves the conversion of the kinetic energy present in the wind into mechanical energy. The extraction of the wind's kinetic energy is accomplished by a blade-rotor system. The mechanical energy which is in a form of rotation of a shaft connected to the rotor system is then converted to electricity using a generator. Normally a gearbox (planetary or parallel design) is employed between the main shaft and the generator to step-up the shaft's speed to the electric generator. As applied to the solar resource, the wind energy available around the planet at any instant is quite vast. However, much of it is outside the earth's surface and beyond the accessibility of current conversion technologies, and would require enormous investment in R&D of the conversion devices (or wind turbines) to extract much of the wind resource potential [10]. Figure 2.2 shows a schematic diagram of a typical utility-scale wind turbine. The nacelle houses the mechanical and electrical controls which include a rotor brake, a mechanical

gearbox and a generator. A yaw mechanism is used to rotate the nacelle and the rotor system to face into the wind.

The U.S. use of wind power for electricity generation has been growing steadily. In Figure 2.3 the annual cumulative U.S. installed capacity growth of wind power is presented. The total U.S. wind installation as of first quarter of 2011 was 41,400 MW representing over 21% of global wind capacity [11]. Figures 2.4 and 2.5 present the U.S. wind power capacity installations (MW) by state in 2010, and the corresponding percentage of electricity generation by state in 2010. Thirty-eight (38) states have utility-scaled wind power installations, with the state of Texas leading by installed capacity with 10,085 MW while the state of Iowa leads by percentage of electricity generation with 15% [11].
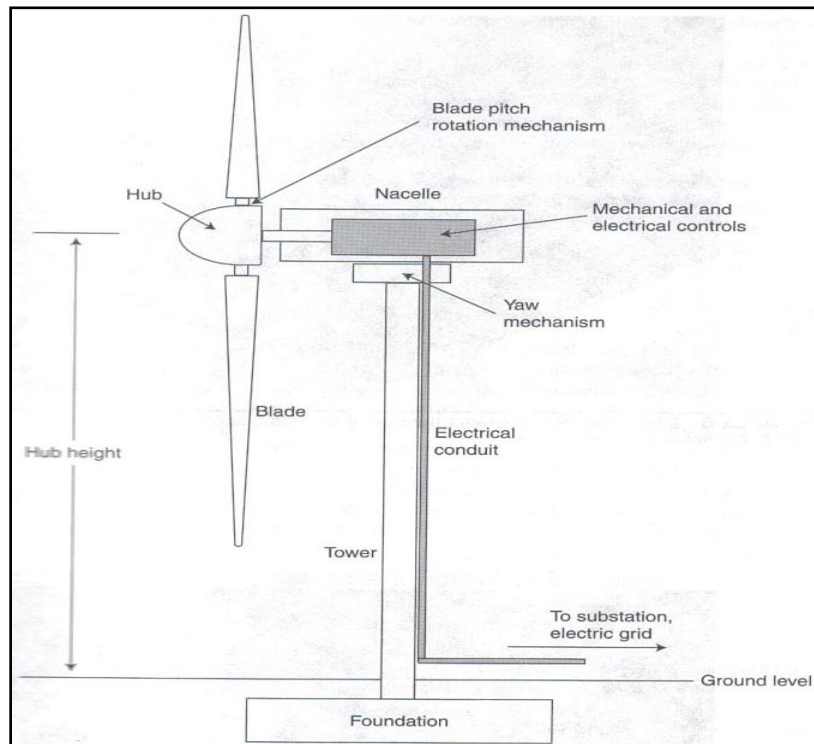
Figure 2.2: Main parts of a utility-scale wind turbine [10]
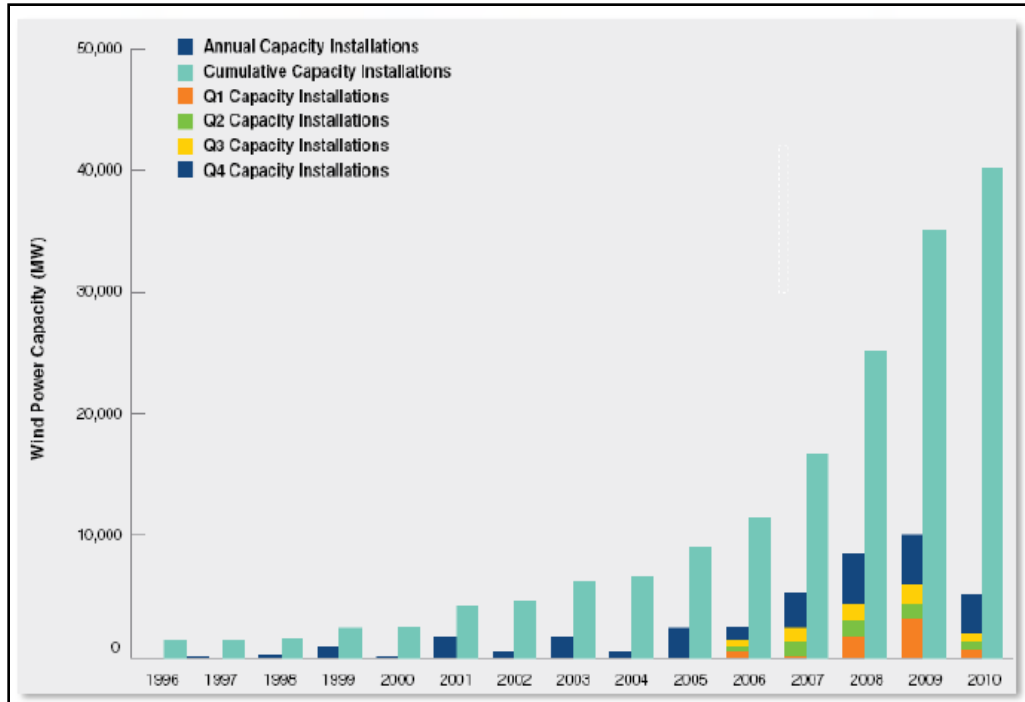
Figure 2.3: U.S. Annual and cumulative wind power capacity growth [11]
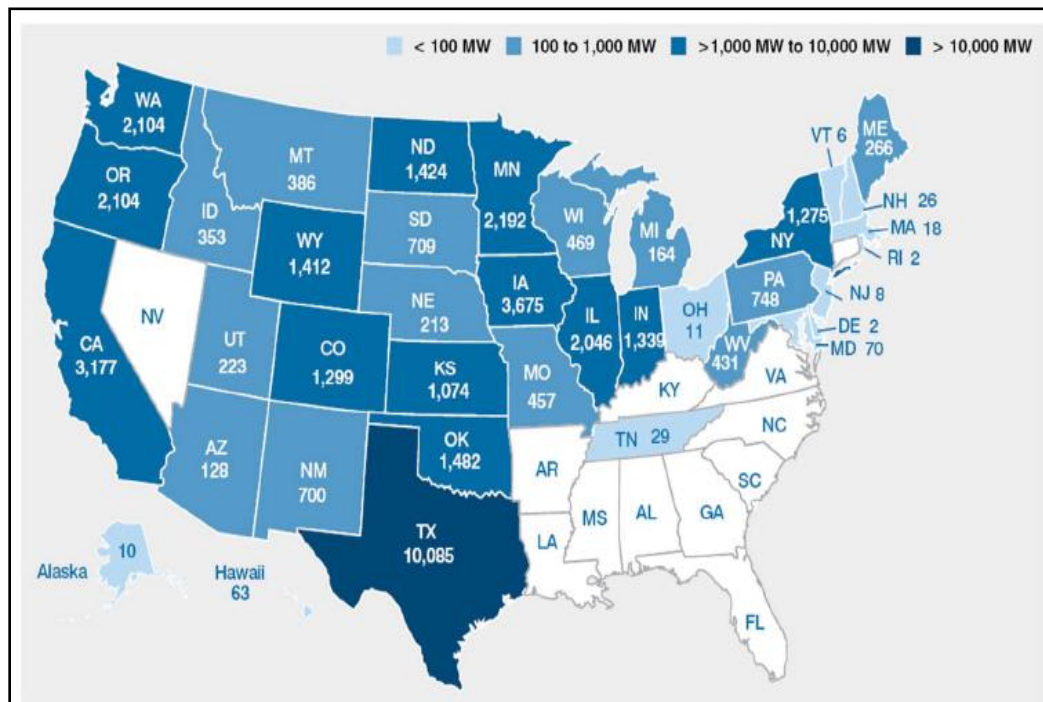
Figure 2.4: U.S. wind power capacity installations by state in 2010 [11]
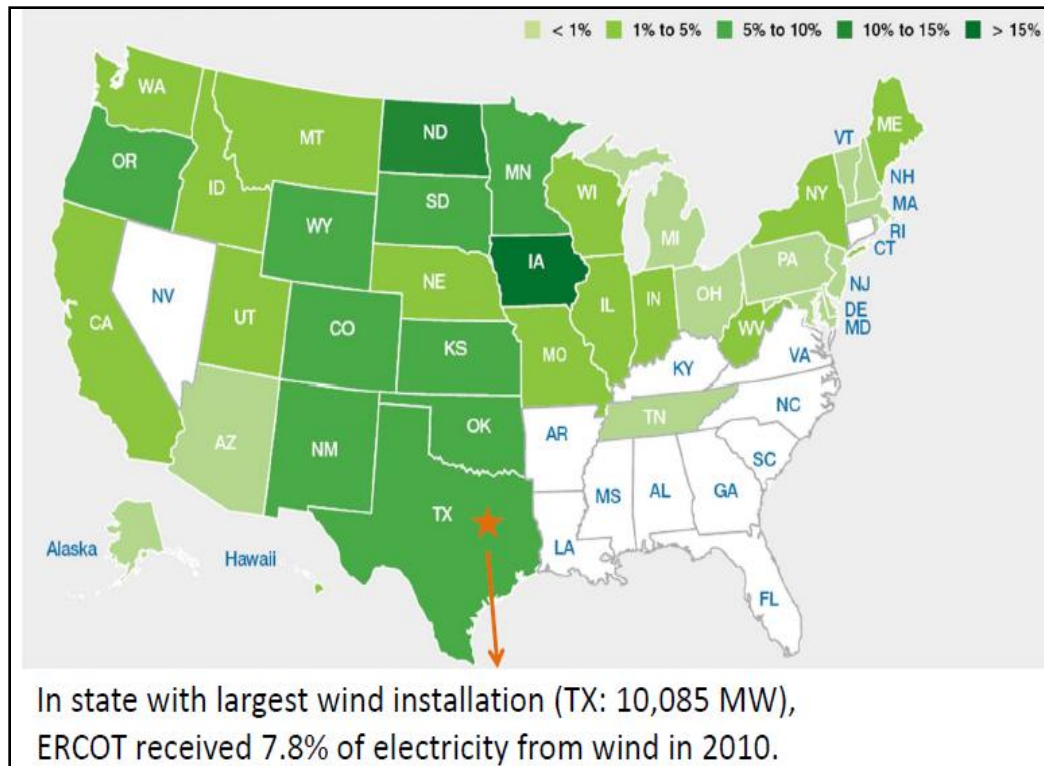
Figure 2.5: U.S. wind percentage of electricity generation by state in 2010 [11]

2.2 Overview of energy storage technologies

The variable nature of the energy output from most renewables oftentimes creates a mismatch between electricity demand and supply. This mismatch can however, be minimized or bridged by the use of energy storage. The use of energy storage can also benefit renewable energy electricity generation by providing the level of power quality and reliability required by the demand side. Moreover, energy storage can provide emergency power and peak shaving opportunities [12].

Technologies for energy storage come in a variety of forms but mainly in chemical, mechanical and thermal. Following is a list of some of the promising energy storage technologies

2.2.1 Pumped hydroelectric storage (PHS)

Pumped hydroelectric storage stores potential energy from height differences in water, however, with the ability to pump water from the lower reservoir to the upper reservoir. As of now it is the dominant form of energy storage in terms of installed capacity forming about 97%. It has a relatively high cycle efficiency (65 -85%), large power capacity (100 – 1000 MW), large storage capacity (1-24+h), long life (30 – 60 years) and a low cycle cost ($0.1-1.4/kWh) [12,13].

2.2.2 Compressed air energy storage (CAES)

Compressed air energy storage refers to storing energy as the potential energy of a compressed gas [14]. Typically, CAES system uses existing underground site (e.g. a salt dome, a rock cavern or an abandoned mine) to store gas at approximately 4-8 MPa at near ambient temperatures and thus, resulting in relatively smaller storage reservoirs [13,15]. During off-peak times, air compressors are operated to pump air into the cavern, which is then expanded through conventional gas turbines during on-peak grid demand. Oftentimes, natural gas is employed concurrently during the expansion process to maximize the energy output from the compressed air [14].

Currently there are two CAES plants in the world that make up the worldwide 400 MW capacity of this energy storage technology. The first system installed in 1978 is in Huntorf, Germany with a capacity of 290 MW for ~2 h. The second plant built in 1991 is found in McIntosh, AL, USA with a capacity of 110 MW for 26 h. Characteristically CAES has large energy storage capacity, high power capacity (50–300 MW), a quick start-up (9 min emergency start, 12 min normal operation), a long storage period (over a year), and a relatively high efficiency (60–80%) [13].

2.2.3 Battery storage (including the flow batteries)

This type of energy storage is achieved through a reversible chemical reaction in accumulators. Chemical energy generated by the electrochemical reactions is transformed into electrical energy and vice versa. Batteries are typically classified on the basis of the accumulators employed, such as lead-acid, nickel-cadmium, sodium-sulphur, lithium-ion, etc. It is a relatively matured technology having good energy densities (up to 150 and 2000 Wh/kg for lithium) [15]. However, their durability decreases considerably for high-amplitude cycling.

To decouple a battery's energy storage capacity from its power capacity and depth-of-discharge, a type referred to as 'flow battery' is employed. An illustration of this type of energy storage is shown in Figure 2.6.
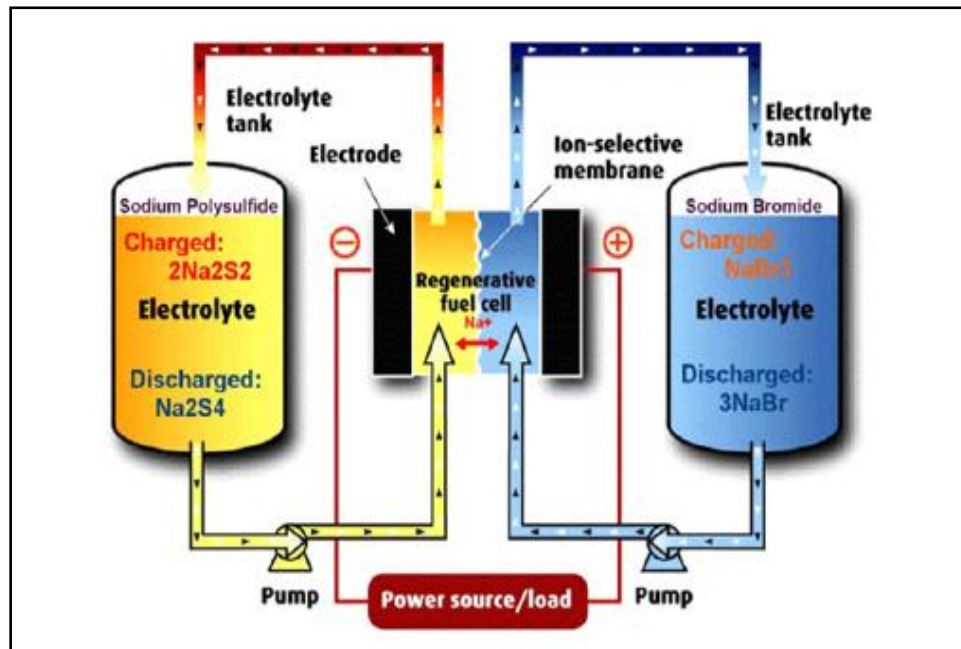
Figure 2.6: Illustration of polysulfide bromide flow battery [15]

With this type, at least one of its liquid electrolytes is stored in external tank and flows through a rector to store or generate electricity. In addition to the flexibility derived with this form, it has a quick response time, deep discharge capability and electricity storage efficiency of about 75% [13,15].

2.2.4 Hydrogen energy storage

This energy storage technology comprises three key components: electrolyzer, storage tank and fuel cell. To generate the hydrogen fuel, an electrolyzer is employed to decompose water into hydrogen (H_2) and oxygen (O_2) gas by introduction of an electric current. The hydrogen gas is then stored in a pressurized tank serving as a buffer between demand and supply. During time of need a fuel cell is used to generate electricity from the stored hydrogen and oxygen from air [13,15].

2.2.5 Flywheel energy storage

Flywheels use the mechanical inertia of a rapidly rotating disc attached to a motor or generator to store or retrieve energy depending on the rotational velocity. Although not widespread, it is a promising technology because of its long life of 15–20 years, long full cycle lifetimes range from 10^5 up to 10^7 and high cycle efficiency of about 90% [16]. However, flywheel energy storage is tempered by high capital cost in the range of $1000-5000/kWh, and also a high self-discharge rate between 55% and 100%/day warranting the use of magnetic bearings and placing the flywheel in a vacuum [16]. Current applications are in the area of uninterruptible power supply, power conditioning and pulse power, and are beginning to be used with intermittent renewable energy sources.

2.2.6 Thermal energy storage (TES)

Another variant of energy storage referred to as thermal energy storage, holds quite a promise for utility-scale renewables especially in the context of solar thermal electric plant. This system uses molten salt or other thermal storage media to retain a high temperature thermal store from sun heat (employing concentrating collectors) for later use in electricity generation.

A comprehensive review of the characteristics of electrical energy storage systems for stationary applications can be found in [15,17-19]. Highlights are the different electricity storage techniques and their field of application (such as permanent or portable, long- or short-term storage), properties and uses of storage for enhancing the grid penetration of intermittent renewables.

2.3   Progress in research on utility scale hybrid power systems

In Chapter 1 attention was drawn to the concerns about the operation of the existing electricity grid structure with large scale deployment of intermittent renewable. A number of research studies aimed at addressing some of the concerns have been undertaken.

Among them is U.S. Department of Energy (DOE) sponsored study entitled *20% Wind Energy by 2030: Increasing Wind Energy's Contribution to U.S. Electricity Supply* [20]. The study explored the impacts and considered specific needs and outcomes in the areas of technology, manufacturing and employment, transmission and grid integration, markets, siting strategies, and potential environmental effects associated with a 20% wind energy penetration scenario. The authors did not find significant technical barriers to

reaching 20% wind energy penetration in the continental U.S., however, they noted that it would require some enhancement of the grid transmission system in such a scenario.

A study on the large scale renewable energy use in the western corridor of the USA, entitled *How do Wind and Solar Power Affect Grid Operations: The Western Wind and Solar Integration Study* [6] has been undertaken by the U.S. National Renewable Energy Laboratory (NREL) and with other partners to examine the operational impact of up to 35% penetration of Wind, Solar Photovoltaics (PV) and Concentrating Solar Power (CSP) on the WestConnect group of utilities (as shown in Figure 2.7) comprising Arizona, Colorado, Nevada, New Mexico, and Wyoming. The investigators concluded that 35% renewable energy penetration is operationally feasible provided significant changes to current operating practice are made, including balancing area cooperation and sub-hourly generation and interchange schedule. This and its partner study, the Eastern Wind and Transmission Study, form the largest solar and wind integration study to date [6].

Figure 2.7 Partial map of western U.S. showing the WestConnect grid [6]

Parson et al. [21] compared the analytic frameworks from recent technical investigations of grid ancillary service impacts of wind power as applied to Xcel Energy (in Minnesota), PacifiCorp and the Bonneville Power Administration (both in the northwestern United States), and discussed the implications and cost estimates of wind integration. The authors noted that although the approaches vary, three utility time frames namely regulation, load following and unit commitment appear to be most at issue. Their findings were that there would be significant impact on power system operation and costs at relatively large-scale wind generation, but at penetration rates that are expected over the next several years these impacts and costs are relatively low. Such cost on the Bonneville Power Administration (BPA) is shown below.

Table 2.1: Cost of integrating 1000 MW of wind into the BPA system [21]

Service	Integration cost ($/MWh of wind production)
Day-ahead forecasting error	1·00–1·80
Load following	0·18
Regulation	0·19
Total	1·37–2·17

Weisser and Garcia [22] focusing on medium-sized diesel-based electricity grids reviewed key concepts concerning supply reliability and power quality at high wind penetration in such grid system. They noted that for questions about the grid stability to be addressed sufficiently, one must undertake a detailed study of the mechanical and electro-magnetic interactions between the wind turbines and the grid. The authors concluded that high wind penetrations in autonomous wind–diesel power systems pose a threat to power quality. However, the level to which the grid can absorb of wind penetration depends on factors such as turbine type, grid strength and prime mover (e.g.

diesel generator) responsiveness. Successful operation of medium-scale systems with wind penetrations (power) of up to 30–40% is reported without the need for special control measures. However, as power control concepts mature the limit on penetration may become less stringent [22].

To meet the stochastic demand in power systems, generation has to be continuously adjusted to meet the varying demand, thus leading to the decomposition of demand into typical and variable parts, and corresponding generating units into base-, demand following-, and regulating units. However, the degree to which load following and regulating capacity need adjustment as wind capacity on the system increases depends on several factors [23] such as size and type of the capacity reserve already on the system, the magnitude of aggregated wind output and demand fluctuation, and the legal criteria that specify the reliability of the power system. Other alternatives to adjusting the demand following capacity and ramping duty are the use of energy storage and/or demand side management measures [23].

Stodola and Modi [24] addressed the question of how much electric load can be substituted by solar electricity without requiring electric energy storage. Moreover, they considered a system that permits 95% of the annual PV output without reducing the base load plants generation since the base load plants have quite a low operating cost as compared to solar power generation. Using historical solar resource data and load data for 2005 from 32 regions of the United States, they concluded that 7.8% of the total annual electric demand could be met by installing 59 GW of PV panels without significant investment in grid infrastructure.

Denholm and Margolis [25] evaluated the limits of large scale solar photovoltaics (PV) in a conventional grid system using the data from the Electricity Reliability Council of Texas (ERCOT) in the year 2000 as a case study. Their focus was to evaluate the ability of PV to provide up to 50% of the grid system load demand by comparing a simulated PV system output to the its usable output. The authors noted that the limited flexibility of the base load plants and thus, the grid results in significant amounts of unusable/excess PV output when PV provides about 10-20% of the system annual energy demand. Several metrics were developed to analyze the excess PV output. Moreover, the limited coincidence of the daily peak solar PV output and the peak energy demand is also a contributing factor to the high levels of unusable PV generation [25].

Solomon et al. [26] examined the grid matching capabilities of wind generation and solar PV generation as applied to the Israel Electric Corporation (IEC) grid system. Their analysis was based on the IEC load data for 2006 and a corresponding simulated hourly performance of PV power and wind power plants in the Negev Desert. Their major objective was to test the hypothesis that wind-PV hybrid system can achieve higher levels of energy penetration and improve matching than either system type alone. Based on the results from the analysis they concluded that due to the differences in diurnal and seasonal output profiles of PV and wind power generation, their combined deployment significantly improves grid penetration compared to their use individually. The authors also reported that they did not find a significant increase in PV grid penetration for the geographical dispersal of the PV plants throughout the Negev Desert as compared with large, single-site plants. However, they concluded that the dispersal strategy would reduce the grid ramping requirements.

Focusing on Europe, Heide et al. [27] investigated the design of a future European electric power system for the case of a highly renewable energy penetration in the search for answers to some key questions such as: How much wind, solar, hydro and geothermal power is good for Europe? Is there an optimal mix between them? How much storage and balancing are needed? Aggregating the renewable power generation over Europe, they found that there exist strong seasonal behaviors between the wind power and solar power, with wind power generation being stronger in the winter than in summer and vice versa for solar power generation. The authors based their analysis on a 100% wind-plus-solar-only scenario assigning the reason to the expected dominance of wind and solar power. Using load, solar and wind time series data (between 2000 and 2008) on a monthly resolution, the corresponding time series mismatch energy between load demand and supply generation was evaluated. The optimal mix was then found from the minimum of the standard deviation of the mismatch energy as a function of varying solar and wind power capacities. The investigators concluded on a seasonal optimal mix of 55% wind and 45% solar power generation weighting to supply the grid demand, and further remarked that for less than 100% renewable scenarios the fraction of the wind power increases and that of solar power decreases.

To address the question of the required size and properties that electric energy storage should have in order to enhance grid penetration of large PV systems, Solomon et al. [17] considered the Israel Electric Corporation (IEC) grid system for their analysis and used the hourly generation data for 2006. Evaluating the needed energy storage capacity for the IEC grid system with PV generation, they constrained the storage system losses to only that of the storage inefficiency (charging/discharging). With this constraint a

22

revealing linkage was observed between the energy and power capacities of the storage, PV system size, and the aggregate effect on the grid penetration. The energy capacity was seen to increase exponentially with PV capacity additions. They reported that at high grid flexibilities in the range of 80% -100%, the PV annual energy penetration of 60%-90% could be achieved. To reduce the size/energy capacity requirement of the energy storage they considered strategies such as PV energy dumping and base-load rescheduling.

CHAPTER 3

METHODOLOGY

This section highlights the logical framework with which the analysis was carried out. Also, the load data as well as the solar and wind resource data used are presented. Key to simulating a typical performance of photovoltaic or wind electric power generation system is a large weather data set with good spatial and temporal resolution over the study area [27].

3.1 Data Sources

3.1.1 Load

Here the characteristics of the grid load are examined. The data given in 30-min time-step was processed to an hourly resolution, and afterwards normalized to the annual hourly peak demand. In Figures 3.1-3, the load data in various forms are presented. Figure 3.1 shows the load duration curve in fraction of the annual peak load. As can be seen from that figure the minimum grid demand (indicated by the dashed line) was approximately at 28% of the annual peak, and for about half of the year the grid was loaded at 40% of the annual peak.

The annual peak load for the given demand profile (of 2008) was about 5.525GW occurring in the month of July. Be advised that all the input time series data for the load, solar PV and wind outputs are normalized to this peak load. Consequently, the analysis

results are multiples or fractions of this peak load unless stated otherwise. The intent is to place the analysis in a more generic form.
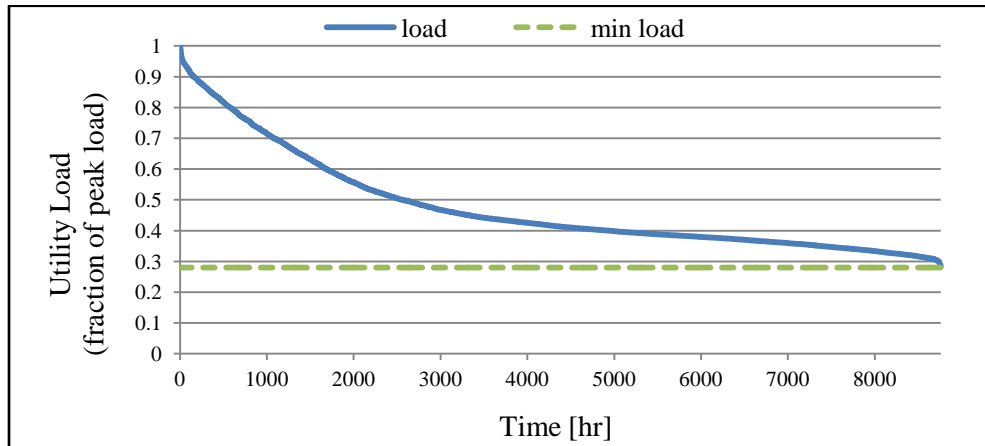
Figure 3.1: Utility annual load duration curve

In this work the months are grouped into four seasons, namely *Spring* (from March to May), *Summer* (from June to August), *Fall* (from September to November), and *Winter* (from December to February). Figure 3.2 shows the daily minimum and maximum, as well as the average daily grid loads for the year.
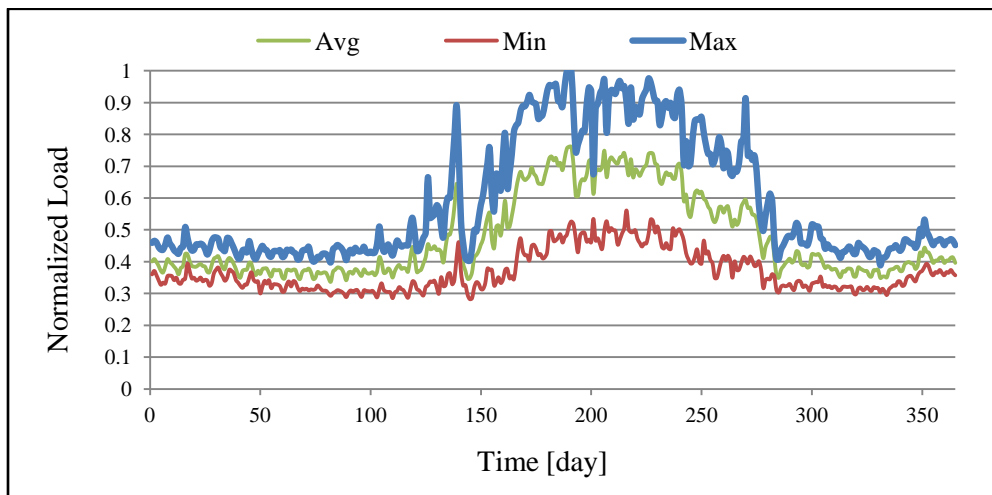
Figure 3.2: Utility daily load variations

From Figure 3.2 we see that the grid experiences a relatively large daily load variation between the minimum and maximum in summer months. This variation averages over 40% as compared to 10-20% for other seasons. Analyzing the seasonal load data in terms of average diurnal variation as shown in Figure 3.3 gives another insight to the load characteristics.
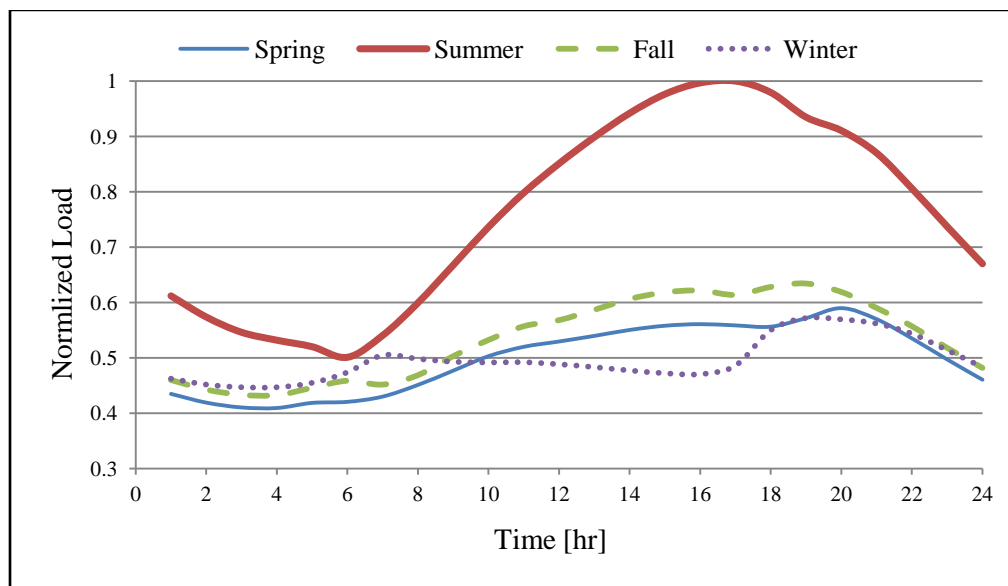
Figure 3.3: Qualitative comparisons of seasonal average diurnal loads

The summer load is observed to peak in late afternoon. This pattern is as expected of a typical southwestern desert location because in such areas the summer loads are mainly driven by air conditioning needs as already mentioned. The winter load profile is seen to have two peaks within a day. These peaks result from evening lighting requirements in addition to heating needs in the morning.

3.1.2 Photovoltaic Power Generation

NREL's Typical Metrological Year 3 (TMY3) weather data set for Las Vegas (Longitude = 115.1°W, Latitude = 36.1°N) was used for simulating the hourly photovoltaic power generation. It was assumed that solar radiation over the study area is similar to that of the measurement location. Practical non-tracking photovoltaic systems are oriented at particular azimuth and elevation angles so as to optimize the power output.

Although there are many orientation strategies to choose from, the most prudent choice is generally dictated by the time need of the energy. Moreover, to an electric power utility, maximizing photovoltaic power output at noon time may not necessarily be of primary importance if its grid peak load occurs at another hour besides noon (usually later in the day). Thus, for utility peak load shaving or load leveling with photovoltaic power generation, a prudent strategy would be to maximize the photovoltaic output at or close to the hour of peak demand [28]. This is achieved by changing the array or collector surface azimuth and elevation angles. However, it is instructive to note that such strategy would result in a lesser annual energy output as compared to the rule of thumb optimal position of south-facing latitude-tilt orientation (if located in the northern hemisphere).

Using NREL's Solar Advisor Model (SAM 2010) [29], a 1 MW photovoltaic power plant (based on silicon cells) was simulated for a Las Vegas location for different orientations using a derate factor (i.e. the conversion efficiency from DC to AC power) of 0.8. It was found that the array orientation (azimuth = 190°, surface elevation = 15°) maximizes the average summer output, however, its peak generation was also found to be at noon as shown in Figure 3.4.
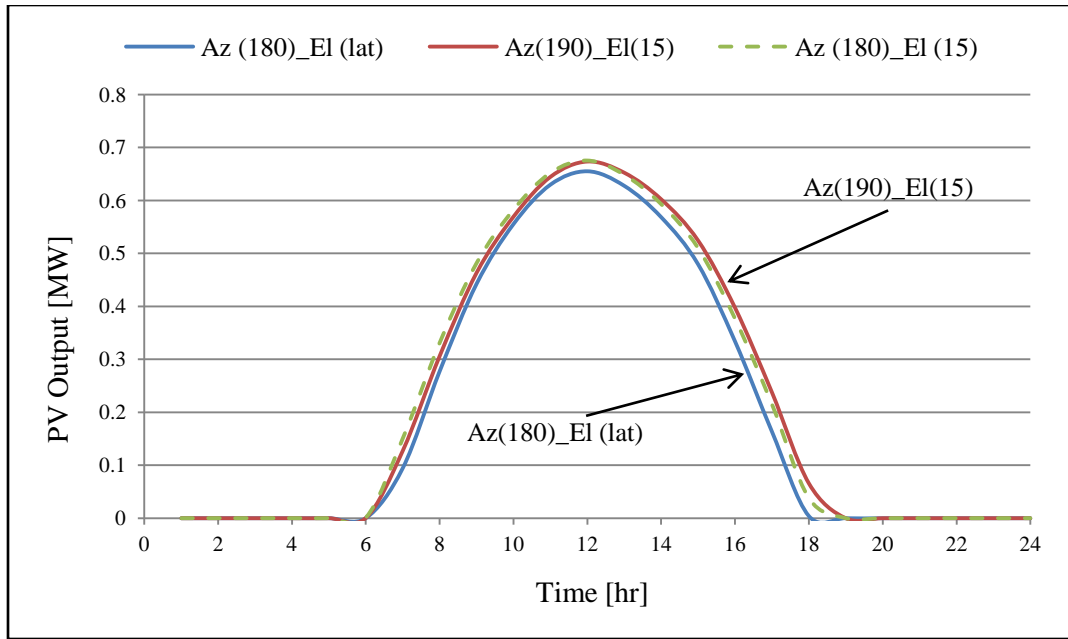
Figure 3.4: 1 MW PV output comparisons for three orientation strategies in summer

A screenshot of the user input interface is shown in Figure 3.5.
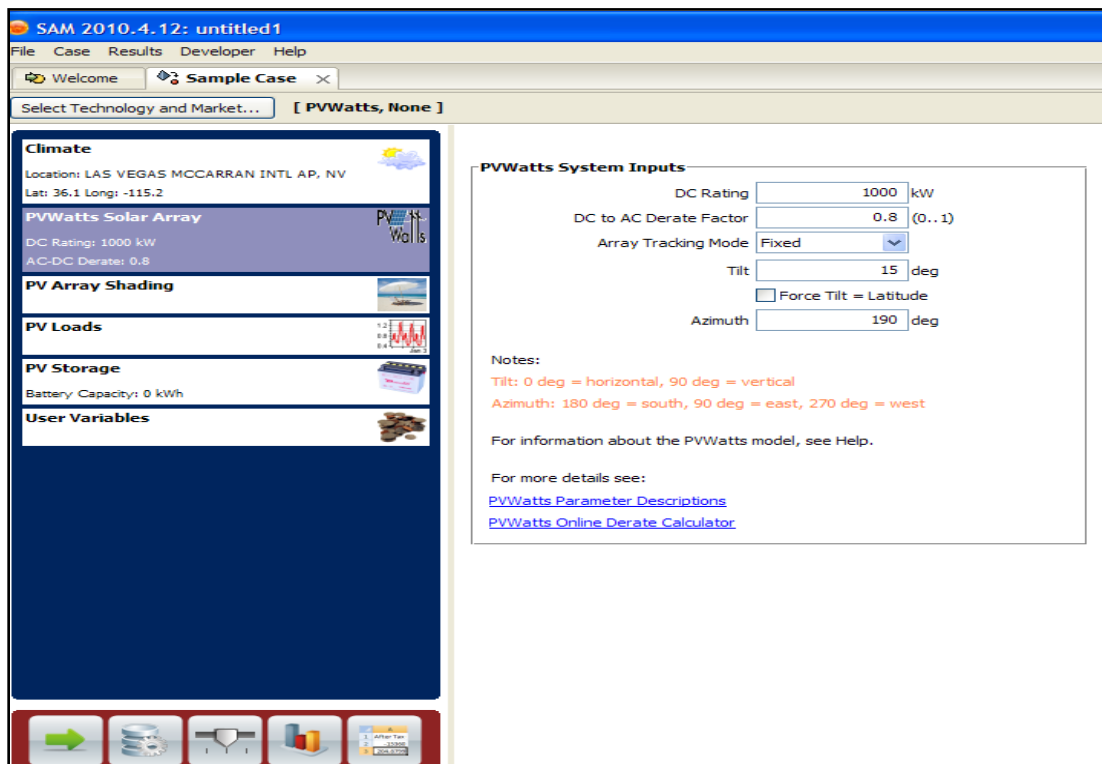
Figure 3.5: A user input interface [29]

3.1.3   Wind Power Generation

NREL/3TIER Group modeled wind data set was used [30]. This modeled data set is for the period spanning 2004 to 2006, and has a spatial resolution of 2-km x 2-km grid cells and temporal resolution of 10-minutes. It includes the wind speed at 100 m height above ground and the wind turbine power output of an assumed 30MW (10 of 3MW wind turbines) wind farm per grid cell. The wind data as retrieved from the source are presented in Greenwich Mean Time (GMT) and has to be converted to the local time for the analysis. Figure 3.6 is a screenshot of the user interface for acquiring the modeled wind farm data set.
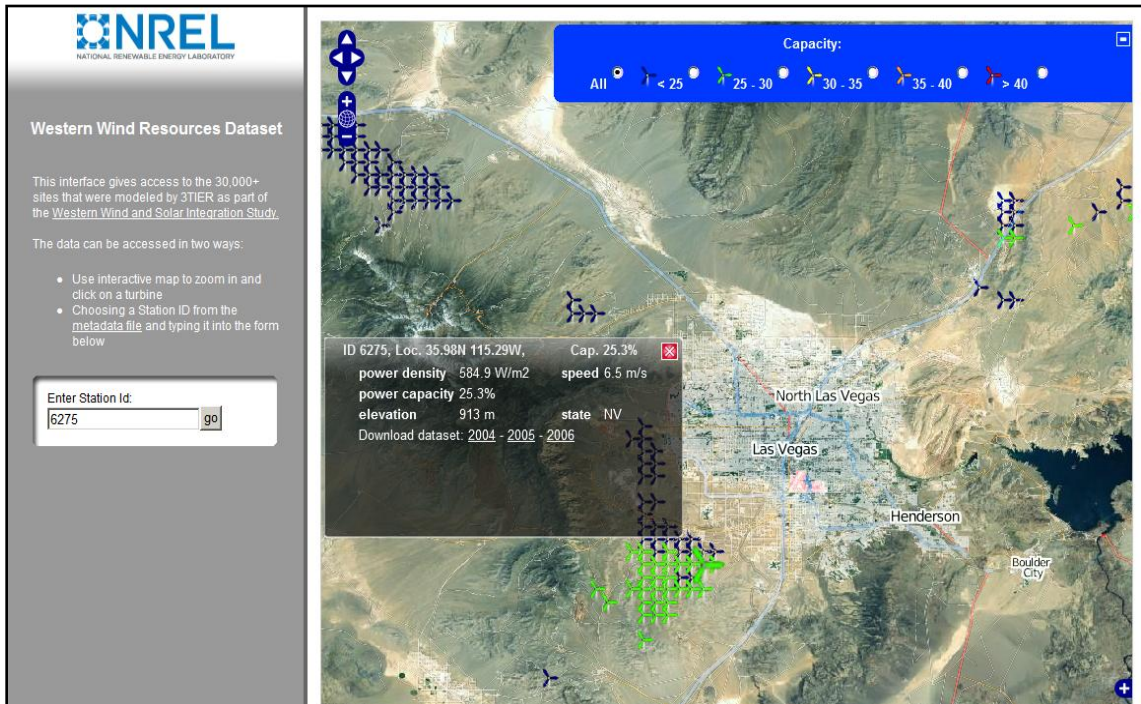
Figure 3.6: User interface for acquiring the modeled wind farm data set

One can obtain the data set by entering the site/station ID in the textbox (bottom left). Then that 30MW wind farm pops up from the group, and from the site summary table

one can download the required year's dataset. For this study ten (10) of the modeled

30MW wind farm sites nearest to the load center were selected and their respective 10-

minute time series values of wind speed and wind turbine power output from 2004 to

2006 averaged. This was done to get a typical wind farm output and wind speed profiles

close to the load center. Then, this averaged 10-minute vector was converted into

average hourly vector. Figure 3.7 shows the selected group of wind farms in the rounded

rectangle.
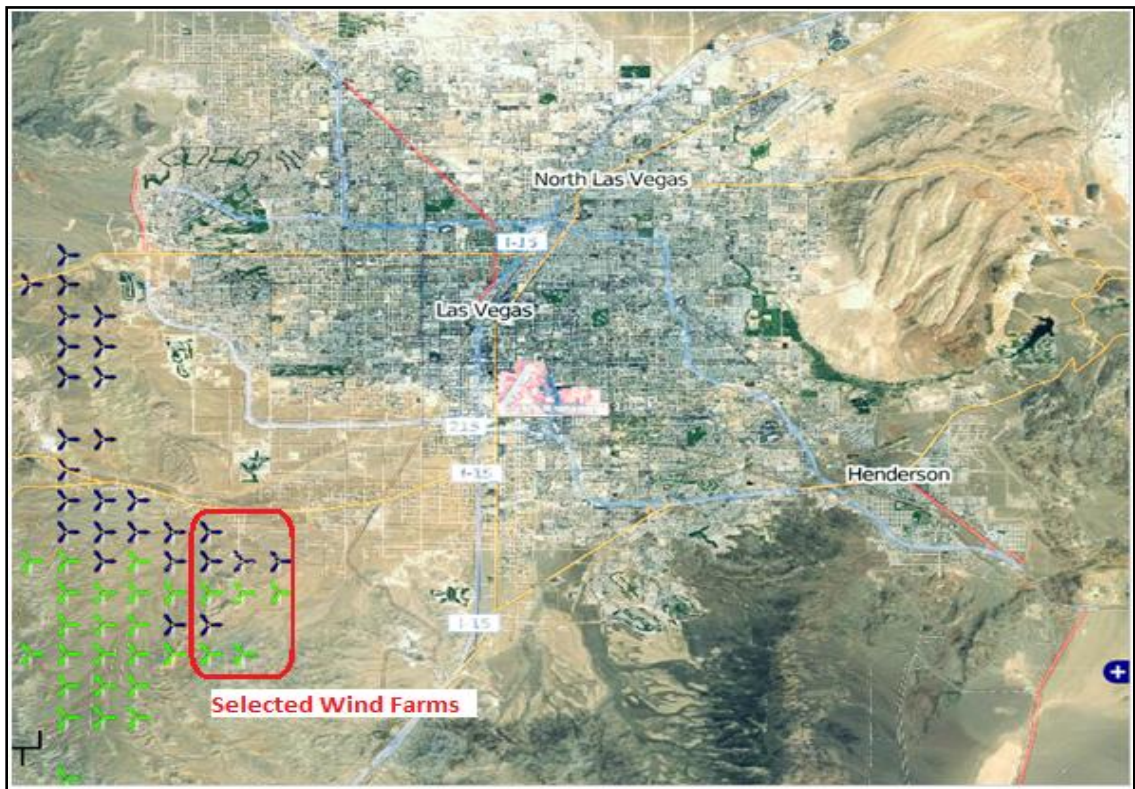
Figure 3.7: Selected wind farms (in rounded rectangle) for the study analysis

Pearson's product moment correlation coefficients between the time series wind

speeds for the selected sites were calculated to determine the directional variations/trends

(i.e. if they do increase and decrease at the same time or vice versa) in the data and thus,

the appropriateness of aggregating that set to estimate the average wind farm profile. Table 3.1 presents the correlation coefficient values obtained.

Table 3.1: Correlation coefficients among the time series power outputs of selected sites

Site ID	6228	6229	6248	6274	6275	6276	6301	6302	6303	6326
6228	1	0.98	0.94	0.93	0.92	0.98	0.91	0.90	0.89	0.88
6229	0.98	1	0.94	0.94	0.93	0.98	0.92	0.91	0.90	0.89
6248	0.94	0.94	1	0.98	0.96	0.97	0.97	0.96	0.94	0.93
6274	0.93	0.94	0.98	1	0.98	0.96	0.97	0.98	0.96	0.93
6275	0.92	0.93	0.96	0.98	1	0.94	0.95	0.97	0.98	0.92
6276	0.98	0.98	0.97	0.96	0.94	1	0.94	0.93	0.91	0.90
6301	0.91	0.92	0.97	0.97	0.95	0.94	1	0.98	0.95	0.97
6302	0.90	0.91	0.96	0.98	0.97	0.93	0.98	1	0.98	0.96
6303	0.89	0.90	0.94	0.96	0.98	0.91	0.95	0.98	1	0.94
6326	0.88	0.89	0.93	0.93	0.92	0.90	0.97	0.96	0.94	1

The correlation coefficient can take values from -1 to +1. A positive value of the coefficient indicates similarity in data trend (1 being the strongest) whereas a negative value shows an inverse/opposite relation. The values obtained for the correlations coefficients as shown in Table 3.1 indicate a close correlation between the wind power outputs of the selected group of sites and thus, justified for using their average to present a typical wind farm output.

3.1.4 Relationships among the grid load, solar (PV) and wind power generations

As mentioned in the preceding section, the relationship between the grid load, solar power and wind power availability can, likewise, be best explained by calculating the

correlation coefficient as presented by [5,31] among them or among their corresponding resources (i.e. wind speed/power density and solar radiation) on which their power outputs depend. The results of the Pearson's product moment correlation coefficients calculation are shown in Table 3.2.

Table 3.2: Correlation coefficient between the grid load (demand) and photovoltaic and wind power generations.

	Load	Solar	Wind
Load	1	0.23	-0.04
Solar	0.23	1	-0.22
Wind	-0.04	-0.22	1

From Table 3.2, it is found that although there exists a complementary potential (negative value of coefficient) between the solar and wind power generations in the study area, the strength is low (-0.22 out of -1). The positive solar – load correlation coefficient indicates some added value of solar PV in matching the grid load profile. Wind power is seen to anti-correlate with the grid load. This is expected in warmer climates, but the magnitude of the coefficient does not define the relationship more clearly for the area under consideration, southern Nevada. The observed low correlation coefficient between the solar (PV) power and wind power availability could mean that when they are deployed in tandem, they may not be as effective (without storage, or as stand-alone system) in meeting/reducing the peak demand, the area of our interest. However, the results of the subsequent analysis of load matching in Chapter 4 would confirm the validity or otherwise of this assumption.

3.2 Development of the Model

A computing algorithm developed using MATLAB for performing an hour-by-hour assessment of photovoltaic-wind-load matching capability and also for determining the storage capacities is described here. In the code/model an Excel spreadsheet which contains hourly data for grid load, the simulated 1 MW photovoltaic system AC output and a 30 MW wind farm AC output is imported. For the algorithm details, refer to the appendix.

3.2.1 Determination of Non-Spilled (NS) Photovoltaic/Wind Capacity

'Non-spilled' photovoltaic/wind capacity denotes a hypothetical maximum capacity photovoltaic/wind system that would not generate more power than the required grid demand during any hour in the year if it were the only supply generation option on the grid. This however assumes a grid flexibility of 100%. Following the method presented by Solomon et al. [32], a non-spilled photovoltaic/wind capacity is determined by first evaluating the ratio of the 1 MW photovoltaic/wind system hourly AC output say ($E_{PV/Wind}$) to the corresponding hourly grid load say (E_{load}) as shown in Eq. (3.1).

$$Ratio\ (i) = \frac{E_{PV/wind}(i)}{E_{load}(i)} \tag{3.1}$$

where i = 1 to 8760 (hours in a year)

The maximum value of this ratio vector is evaluated and the obtained value of the reciprocal of this maximum ratio (*max(Ratio(i))*) gives the capacity of the non-spilled photovoltaic or the wind system.

$$NS = \frac{1}{max\big(Ratio(i)\big)} \tag{3.2}$$

33

For the load profile used for this study, the evaluated non-spilled PV and wind capacities were obtained as 2.376 GW (~ 43% of peak demand) and 1.740 GW (~ 31% of peak demand) respectively.

3.2.2 Sizing of energy storage capacity requirements

In the model the storage system is characterized by the following parameters which are defined as:

- Maximum energy capacity

This is the maximum amount of available energy in the storage system in a fully charged state.

- Minimum energy capacity

This is the minimum amount of available energy in the storage system below which the storage is not discharged to complement supply generation in meeting the grid load.

- Maximum power capacity

This is the maximum amount of energy that can be injected into or withdrawn from the storage system in any instant (or for any hour being the time step in this study). Though maximum power of charge and discharge may be sized differently, the two are set equal for this analysis.

- Cycle efficiency

The product of the charging and discharging efficiencies of the storage system is the cycle efficiency. For this study the charging or discharging efficiency is obtained by finding the square root of the cycle efficiency.

- Total discharge time

This is the duration at which the storage energy capacity is exhausted at maximum power discharge. In the model this is obtained as the ratio of the energy capacity to the power capacity. However, in practical systems this depends on the depth of discharge and operational conditions of the system [15]. Separating the power and energy dimensions of storage systems is not trivial and this presents a challenge in choosing the optimum time constant for most storage technologies.

- Self-discharge

This is the rate at which the storage system intrinsically discharges/loses its available capacity whether it is being used or not. It represents an inherent loss to the storage system. It is dependent though on many factors including environmental conditions

In the model the storage losses are simplified to that of only cycle efficiency (n_{cycle}) and self-discharge. Being guided by other investigators' work [9,17], the cycle efficiency was set at 80% (indicative of battery energy storage) and assumed that of self-discharge rate to be 10% per month of the available energy capacity.

To proceed with the evaluation, a base generation capacity (as a fraction of the peak load) is first defined which sets the minimum (annual or seasonal) conventional plant generation at any hour on the grid. Consequently, the flexibility of the grid is set by this value. During each hour, meeting the grid load/demand is first attempted with the base generation. If thereafter, a net load or mismatch in energy, (say E_{mBase}) exists, the deficit in supply generation is then attempted with the PV/wind generation. Any remaining deficit or surplus in supply generation, (say $E_{mPV/Wind}$) after accounting for the PV/wind output is then pulled from or charges the energy storage. However, the discharge process

is constrained by the minimum storage energy capacity, the maximum power capacity and discharge efficiency.

Figure 3.8 shows a schematic of a typical energy storage integrated hybrid (PV-Wind) grid power system. On the combined load-generation plot, the area indicated by the plus (+) sign is where surplus generations is observed and hence the energy storage being charged. The opposite is true for that indicated by the minus (-) sign.
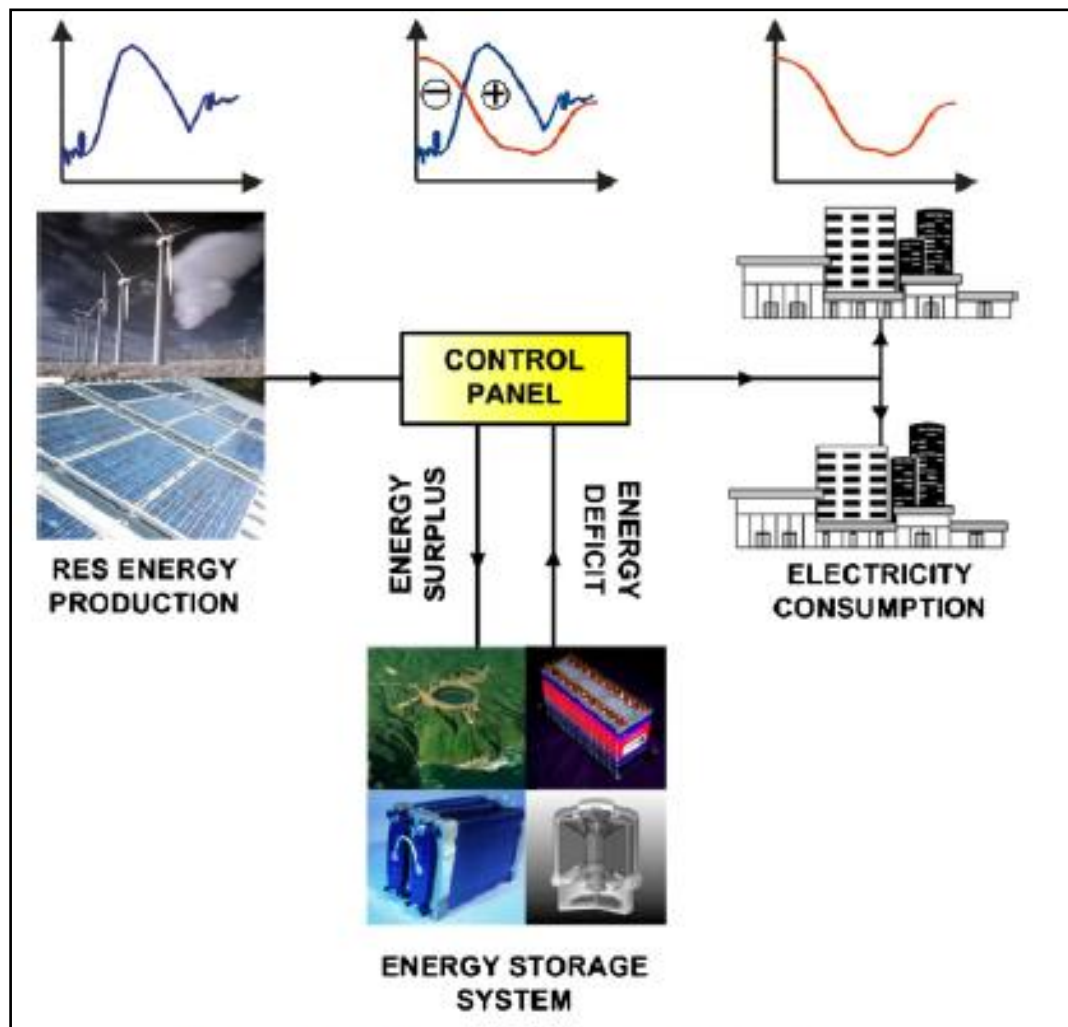
Figure 3.8: Typical PV-wind-storage grid power system [33]

The mathematical description of the charging and discharging process is generally described by Eq. (3.3) below.

$$E_{str}(t) = (1 - DsgRate) \times E_{str}(t-1) + \begin{cases} eff_{chg} \times E_{mPV/Wind} & if\ E_{mPV/Wind} > 0 \\ \dfrac{1}{eff_{dsg}} \times E_{mPV/Wind} & if\ E_{mPV/Wind} < 0 \end{cases} \quad (3.3)$$

where:
- t is time
- eff_{chg} & eff_{dsg} are the charging and discharging efficiencies (which are related to the "cycle efficiency" denoted above)
- *DsgRate* is the self-discharge rate

The time series $E_{str}(t)$ describes the charging level of storage. The difference between the maximum and minimum value of $E_{str}(t)$, however, determines the required storage energy capacity. The storage power capacity is, however, set by the maximum value of time series given by ($eff\_c.E_{mPV/Wind}$ or $eff\_d^{-1}.E_{mPV/Wind}$) [27]. The developed algorithm has the capability of determining among other items the:

- required magnitudes of energy and power capacities of the storage system;

- annual/seasonal energy penetration of PV-wind only and PV-wind-storage system;

- daily net storage energy capacities;

- annual/seasonal peak load reductions for any desired period within the year;

- system energy losses (due to storage inefficiencies and or dumped generations).

The flowchart highlighting the general algorithm steps is presented in Figure 3.9. Definitions of the parameters are presented below. Refer to appendix for detailed descriptions.

- *ChgDsgLoss* is the energy loss due to storage charging and discharging cycles

- H_{t_max} is the storage system maximum power capacity;

- H_{min} and H_{max} are the storage system minimum and maximum energy capacities;

- H_{new} is the current/end of hour storage energy capacity;

- E_{out_RE} is the total renewable energy generation at time t;

- E_{mb} is the resulting mismatch between load and base generation;

- E_{out_dmf} is the demand-following generation on the grid;

- E_{dump_RE} and E_{usable_RE} are the dumped and usable renewable energy generation;

- *StrShare_pk* peak time storage dispatch capacity (refer to Eq. 4.3)
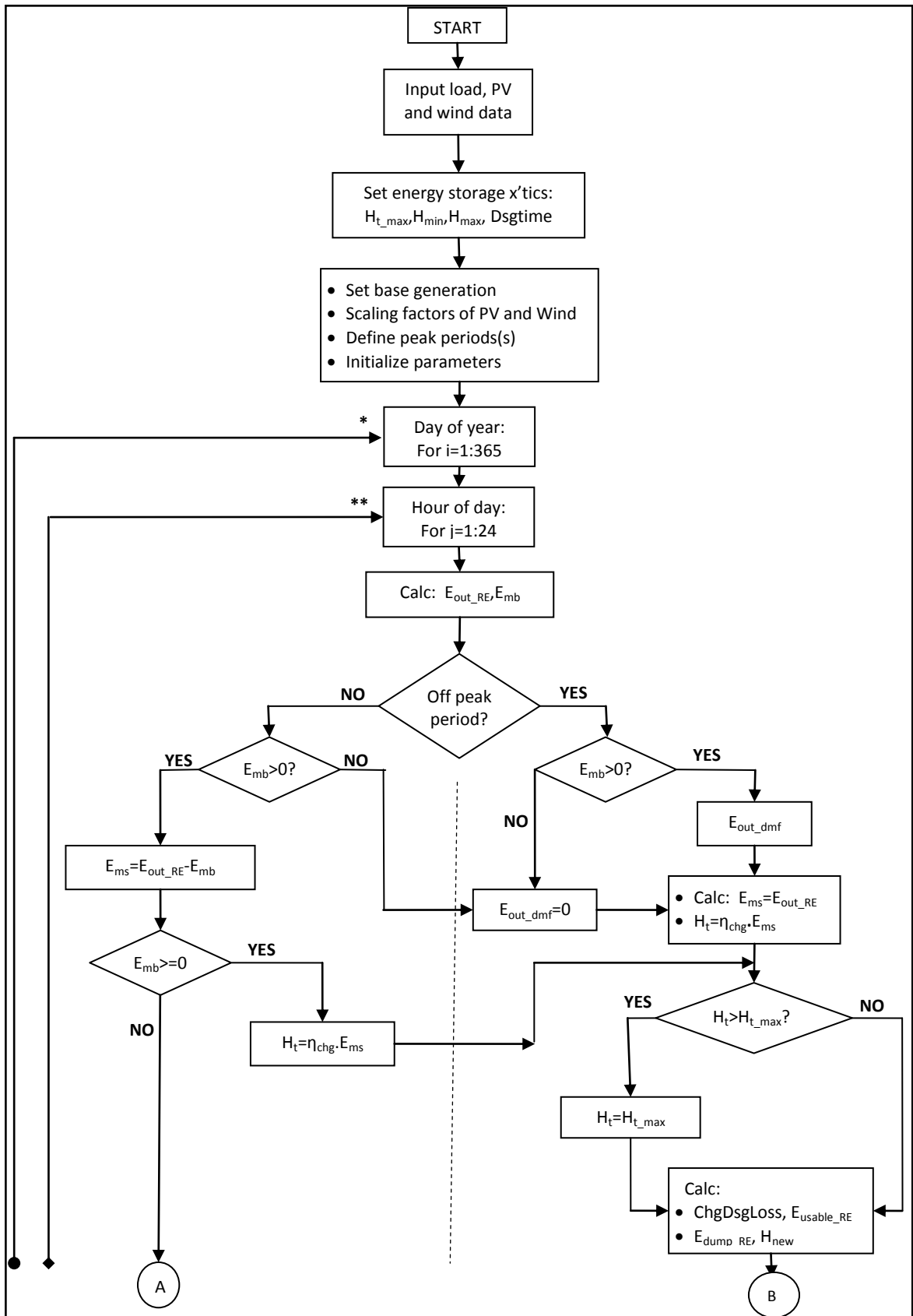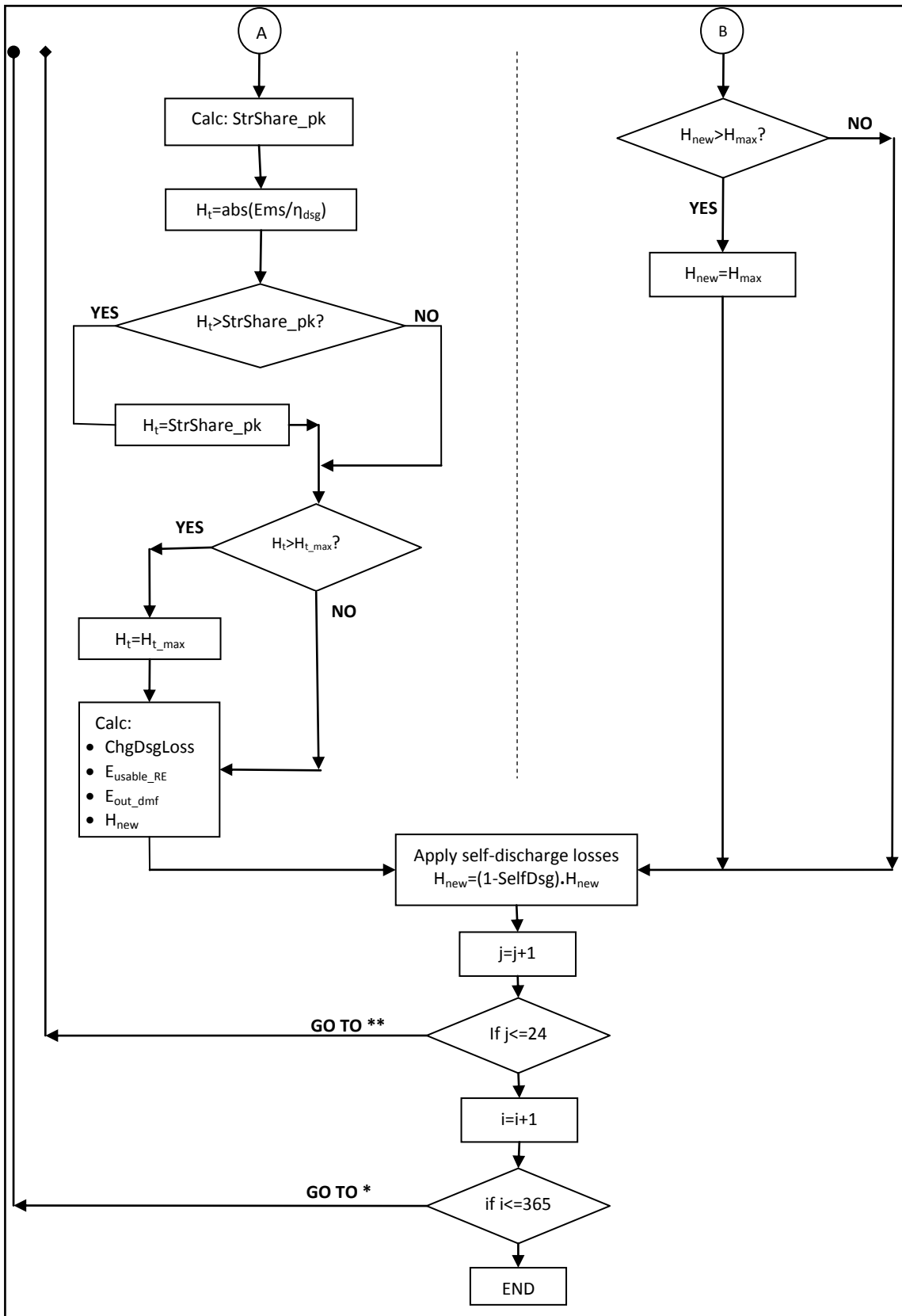
Figure 3.9: Flowchart for the hybrid system analysis

3.2.3 Quantification of seasonal optimal mix between wind and solar

In this section an attempt will be made to quantify an energy-based optimal seasonal mix between wind and solar (PV) power generation based on the given load profile. To begin with such an analysis the diurnal and seasonal variations of the wind and solar power for the selected location/geographical area have to be examined for complementarities. With the time series data (load, wind and solar power generations) quantifying the seasonal optimal combination for a 100% wind-solar scenario becomes a relatively straightforward analysis.

Key to such quantification is to determine the mismatch energy between the grid load and supply generation [27]. For this analysis the mismatch energy is evaluated as given by Eq.(3.4)

$$E_{me}(t) = \frac{L(t)}{L_{max}} - \left[a \frac{S(t)}{S_{max}} + b \frac{W(t)}{W_{max}} \right] \tag{3.4}$$

Where:

$E_{me}(t)$ is mismatch energy during time step t (monthly considered in this case);

$S(t)$ is the total solar energy output during time t;

S_{max} is the maximum total monthly solar PV generation within the considered period;

$W(t)$ is the total wind energy output during time t;

W_{max} is the maximum total monthly wind generation within the considered period;

$L(t)$ is the total demand during time t;

L_{max} is the maximum total monthly grid load within the considered period

Coefficients *a* and *b* define the average fractions or percentage of the load to be served with the solar PV and the wind generations respectively for that demand profile matching. The coefficients are constrained to ($a+b=1$). Varying the values of the coefficients, *a* and *b*, the standard deviation of the mismatch energy is then calculated as a function of ($a=1- b$). Where the minimum of the standard deviation occurs provides an indication of the optimal contributions of the respective energy sources to matching the demand. The algorithm computed in MATLAB is presented in the appendix.

SIMULATION RESULTS AND DISCUSSION

4.1 Dependence of storage capacities on PV system size and base generation

In this section we present the required annual storage energy capacities and the corresponding power capacities requirements for varying sizes of the PV system and base supply generation. Figure 4.1 shows the relationship among required annual storage energy capacity, PV system size and base generation capacity (which determines grid flexibility). *Note that all the values found in the figure are multiples of the annual peak load.*

From Figure 4.1 it is seen that the required energy capacity monotonically increases with increasing PV system size for a given base generation capacity. The increment is observed to be linear for all PV system sizes considered with the base generation capacity range 0-0.07 and partly for base generation range 0.14-0.28. For the latter range, an exponential increment is seen from absolute PV sizes of 0.75 upwards with base generation of 0.21 and approximately 0.35 upwards at base generation of 0.28.
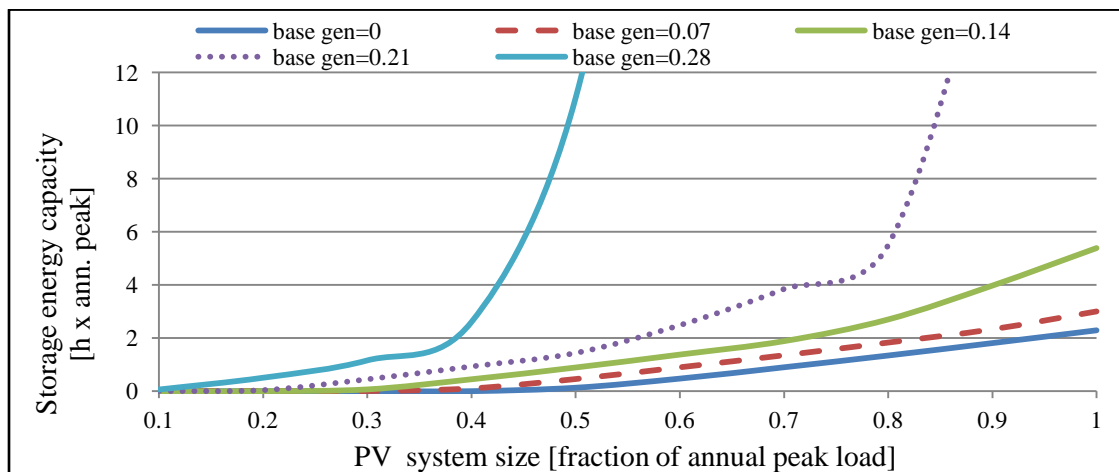
Figure 4.1: Relationship among storage energy capacity, PV size and system flexibility

The region of linear variation seen in Figure 4.1 is where the storage energy capacity need is determined by just the daily peak excess PV generation which charges the storage. The exponential increment is where the storage energy capacity requirement is determined by the cumulative effect of the sum of the net daily stored energies from previous days and the next day's peak excess PV generation [17].

Additional insight into the observed exponential variation of energy capacity in Figure 4.1 can be gained by plotting the net daily storage energy capacities of different PV system sizes as shown in Figure 4.2. It can be seen in Figure 4.2, especially for the 0.6 and 0.7 PV system sizes that the energy capacity monotonically increases between approximately the 75th and the 120th day of the year. This period represents the spring season where grid loads are relatively low while favorable ambient temperature conditions and the sun intensities lead to higher PV generation outputs. As a result of much more surplus PV generation, a larger storage capacity is required to contain these surpluses. This is what results in the exponential increments noted in Figure 4.1 and Figure 4.2
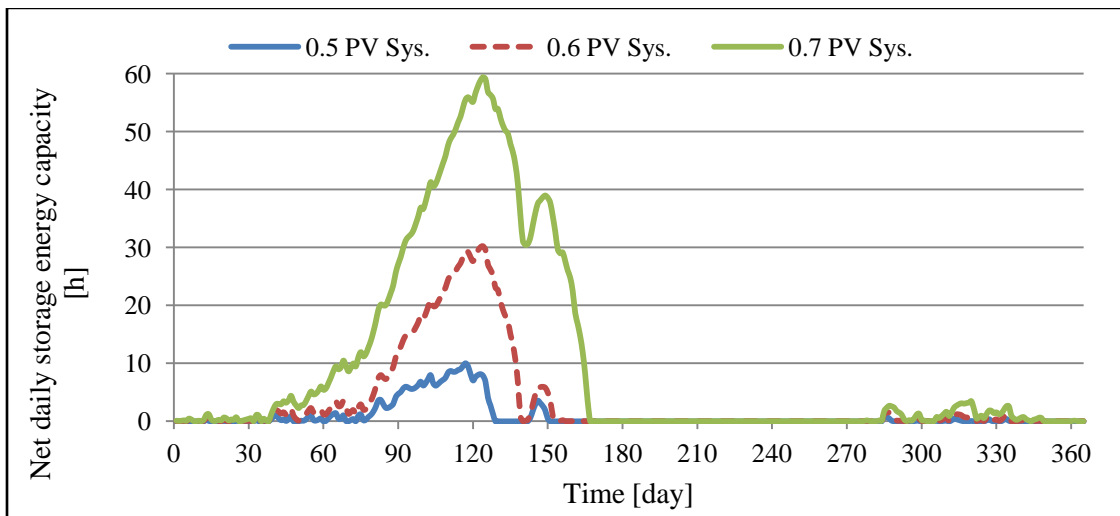
Figure 4.2: Daily storage energy capacities at base generation of 0.28 of annual peak load

Figure 4.2 reveals that for the considered PV system sizes the storage capacity is exhausted during the day's period in the summer season (days 151-243) and early fall (days 243~285). However, it is seen that higher PV system capacities close up the storage 'dry up period' but result in excessively high storage energy capacities. We note in passing that the size of the storage system also depends on the orientation strategy of the PV arrays since higher surface elevation angles generally produce more energy in fall-winter periods and less in summer in contrast to lower elevation angles such as one employed for this study.

Moreover, Figure 4.2 brings to fore some of the challenges that power utilities would likely be faced with higher penetrations of the power grid system with conventional PV systems energy generation. An operational strategy has to be devised to contain these seasonal energy surpluses by this technology in view of ensuring economically utilizable storage sizes. One way of addressing this could be dumping of some generation and/or increasing the flexibility of the grid system.

If we consider no dumping of excess PV generation, then the maximum annual hourly peak value of the energy capacity within the simulated time period is selected as the required storage energy capacity for the given PV system size and with regard to base generation or grid flexibility employed. It can be recalled from Chapter 3 that we defined our power capacity to be the maximum charging or discharging load at any instant/time step within the simulated time period. Thus, as said of the energy capacity, either the annual hourly peak storage charge load resulting from the excess PV generation, or the annual maximum discharge load to meet deficit in grid demand for a given base generation determines the annual storage power capacity requirement.

In Table 4.1, the required annual storage energy capacities and power capacities for different sizes of PV system and for a base generation of 0.28 are presented. As observed for the energy capacities, the power capacities tend to increase with the PV size. The increment in the power capacity could be assigned to the potential of the storage having more of available energy capacity now for discharge to meet the deficits in grid demand. It is instructive to note that having a power capacity value greater than 0.72 (since base generation is considered to be 0.28) is as a result of discharge inefficiency, thus drawing more than actually used to serve the demand deficit.

Table 4.1: Required annual storage energy capacities and power capacities
for different sizes of PV system at 0.28 base generation

PV Capacity	Storage Capacity	
	Power	Energy [h]
0.1	0.01	0.05
0.2	0.08	0.50
0.3	0.15	1.15
0.4	0.23	2.59
0.5	0.31	11.04
0.6	0.63	31.49
0.7	0.63	60.68
0.8	0.72	92.58
0.9	0.72	124.77
1.0	0.74	166.28

Note: all values are multiples of the annual peak load [5525 MW]

4.2 Annual PV system energy penetration with varying base generation

In this work the PV energy penetration is obtained as the ratio of the total usable PV generation to the total grid demand/load. One of the options cited for enhancing the economic penetration of intermittent renewables is by increasing the flexibility of the

electric grid system [9,34]. Figure 4.3 presents a hypothetical 0.5 PV systems annual energy penetration and total energy losses with varying base generation. In the legend, P and L represent energy penetration and losses respectively. The storage system assumed for the following analysis has max power capacity (of 0.5) and max energy capacity (of 10 h).
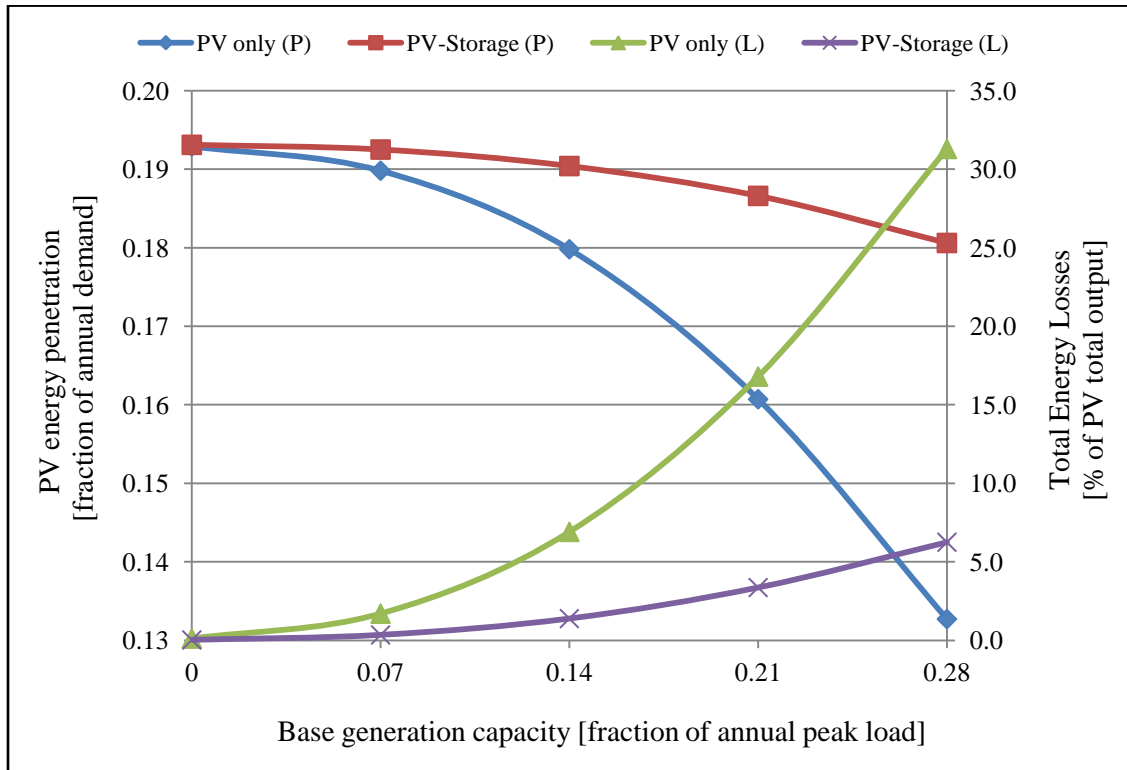
Figure 4.3: Annual PV energy penetration and total losses with varying base generation (PV = 0.5; storage cap [power = 0.5, energy = 10 h])

In Figure 4.3 it is seen that as the base generation increases, thus reducing system flexibility, the PV system annual energy penetration reduces for both the PV-only system and the PV-storage integrated system respectively. However the rate of reduction of the PV annual energy penetration is observed to be less steep for a PV-storage integrated system. Consequently, this confirms that energy storage presents another way through

which PV grid penetration can be increased, which results from the usefulness of otherwise excess/dumped PV generation for a PV-only system.

Superimposed on the PV energy penetration versus base generation plot (Figure 4.3) is the accompanying total energy losses observed for the two PV systems. The PV-only system energy loss is derived from the dumped excess generation whereas that of the PV-storage system is the aggregate of the excess dumped generation, the storage charging and discharging losses. The total energy loss is observed to increase exponentially for the PV-only system as the grid becomes increasing inflexible.

4.3 Relation between PV energy penetration and storage energy capacity

The size (i.e. the MWh or energy capacity) of energy storage technology is the determining factor of the investment cost as opposed to its power capacity (i.e the MW size); the larger the energy capacity the higher the capital cost. Thus, a utility planner would opt for low MWh to MW ratio in sizing of storage capacity [28]. Effectively, this would mean having shorter discharge times. Typical energy-to-power capacity ratio of utility-scale energy storage systems, however, ranges between 4-16 h [9]. It is instructive to note that determining the required energy capacity of storage systems based on losses resulting only from cycle efficiency and self-discharge as had been the case in our previous analysis could lead to a 'wasteful' sizing [34] and would be shown by the subsequent analysis.

Consider a hypothetical 0.5 PV system having integrated energy storage with maximum power capacity of 0.5 of annual peak load (i.e. 0.5 x 5.525 GW). The storage energy capacity is obtained and varied by multiplying assumed discharging times from 1

to 10 hours by this maximum power capacity respectively. The annual base generation is fixed at 0.28.

Figure 4.4 presents the relationship between PV annual energy penetration with corresponding losses and storage energy capacity.
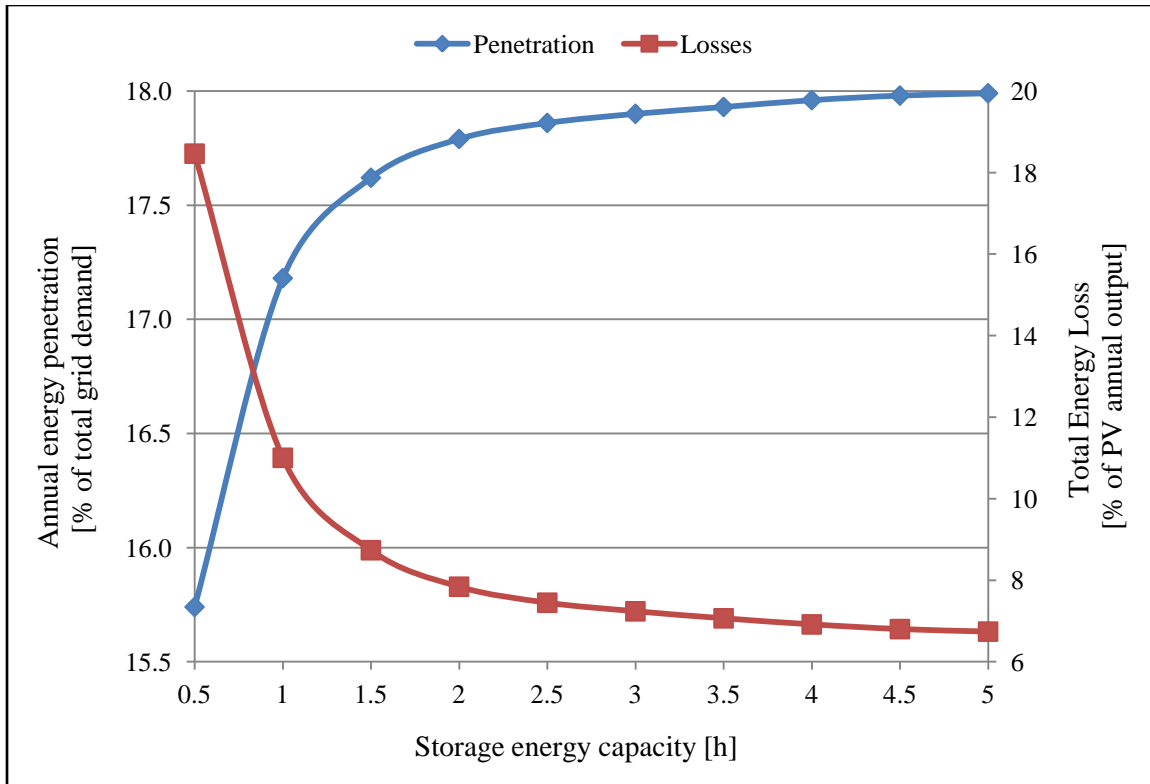
Figure 4.4: Relation between energy penetration and storage energy capacity
(PV = 0.5; storage max. power cap. = 0.5; base gen. = 0.28)

From Figure 4.4 it can be seen that increasing the storage energy capacity beyond the knee region does not offer any significant increase in the PV energy penetration. In fact less than 0.5% difference in annual energy penetration is observed from the previously determined (with no dumped PV generation) larger maximum energy capacity of 11h (and with a corresponding maximum power capacity of 0.31, see Table 4.1 and Figure

4.3) and a storage system with maximum energy and power capacity of 2-2.5 h and 0.5 respectively. However, it is worth to note that the latter storage capacity would result in between 7.5 -7.8% loss of available PV energy generation compared to 6.2% for the earlier storage capacity of (power = 0.31, energy = 11 h).

To refine further the values of the power and energy capacities of the required storage for the given load profile and annual base generation of 0.28 and an assumed 0.5 PV capacity, two boundary conditions were defined. The optimized/minimum storage capacity values (power and energy) should allow for less than 7.5% loss of the annual PV energy output and in addition not less than 17.5% PV energy grid penetration. Based on these two criteria, the energy-based optimized storage capacity was found as (power = 0.25, energy = 2.5 h) resulting in losses of 7.45% and penetration of 17.86%. Figure 4.5 shows the relation among energy penetration, energy losses and storage power capacity observed for the selected optimized storage energy capacity.
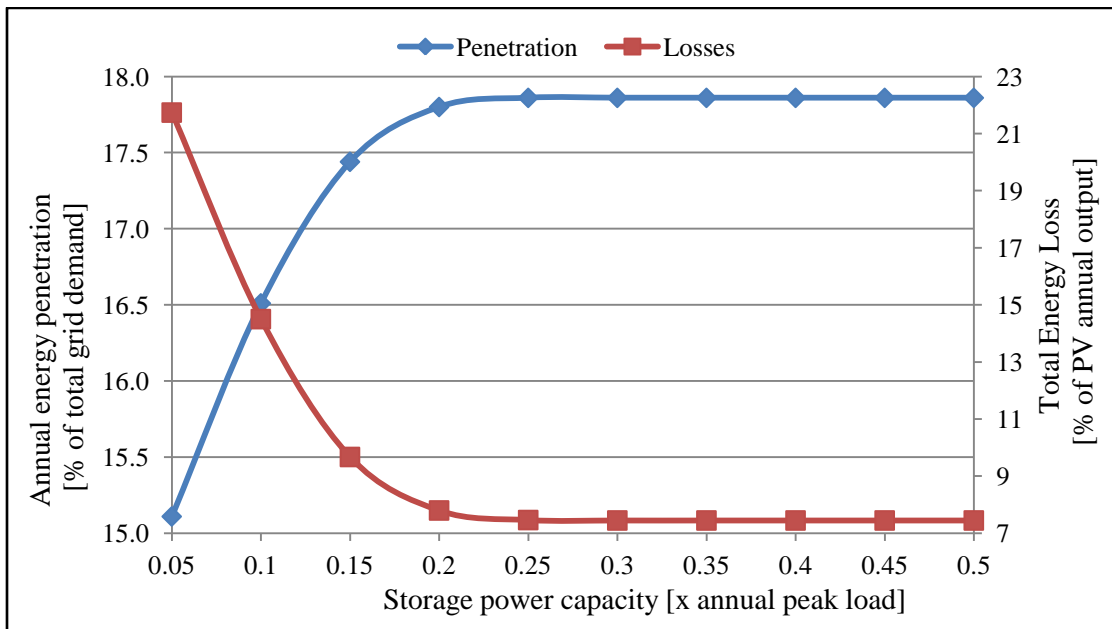
Figure 4.5: Relation between energy penetration and storage power capacity
(PV = 0.5; storage max. energy cap. = 2.5 h; base gen. = 0.28)

The results such as presented by Figure 4.4 and Figure 4.5 could be of significance to a power utility investment decision process on energy storage capacity integration with intermittent renewables. This results from the observation that with a smaller energy-to-power capacity ratio of the same storage technology, potential savings in cost could be realized. However, such a decision will call for additional economic analysis on the associated energy losses.

4.4 Impact on grid peak loads with PV-wind-storage system

4.4.1 Seasonal peaks

Table 4.2 shows the grid seasonal performance characteristics for the different hybrid systems with an imposition of 0.28 base generation. For this analysis, the energy-based optimized storage system capacities (max. power = 0.25, max. energy = 2.5 h) determined in the preceding section for a 0.5 PV system and 0.28 base generation is adopted. Refer to the endnotes at the bottom of the table for the definitions of the hybrid systems.

Here the respective seasonal effects of the energy storage on the integrated storage hybrid system were evaluated by isolating the season's source/input data (i.e. the load, PV and wind power outputs) from the rest. Initializing (i.e. @ t = 0) the available storage energy capacity to zero, the simulation was then executed for that season as a standalone time period. By doing this the net stored energy from the other periods are not brought into it, and thus reflecting the actual season's impact or interactions. From Table 4.2 it is observed that the seasonal peak load reductions and the corresponding energy penetrations, in general, increase with wind and storage integrations with the PV.

Table 4.2: Seasonal performance characteristics of the hybrid systems

	Hybrid System				
	PV[a]	PV-W1[b]	PV-W1-S[c]	PV-W2[d]	
Period	Energy Penetration [%]				Notes
Spring (Mar.-May.)	13.02	16.68	24.09	18.16	Percentage of season's total grid demand
Summer (Jun.-Aug.)	16.07	16.36	16.76	16.39	
Fall (Sep.-Nov.)	13.37	15.60	19.10	16.13	
Winter (Dec.-Feb.)	6.76	10.31	16.69	11.72	
	Peak Load Reduction [%]				Notes
Spring (Mar.-May.)	4.32	6.88	7.69	9.44	Percentage of the season's peak load
Summer (Jun.-Aug.)	5.34	5.59	5.59	4.82	
Fall (Sep.-Nov.)	11.46	12.40	12.57	13.31	
Winter (Dec.-Feb.)	0	5.63	10.61	5.63	
	System Energy Losses [%]				Notes
Spring (Mar.-May.)	51.50	44.77	20.08	45.87	Percentage of the season's total renewable output
Summer (Jun.-Aug.)	3.00	2.94	0.59	4.45	
Fall (Sep.-Nov.)	28.58	23.42	4.98	26.75	
Winter (Dec.-Feb.)	60.32	48.36	15.11	48.87	
	Demand Deficit [%]				Notes
Spring (Mar.-May.)	15.46	11.80	4.39	10.32	Percentage of season's total grid demand
Summer (Jun.-Aug.)	41.35	41.06	40.66	41.04	
Fall (Sep.-Nov.)	24.28	22.05	18.54	21.52	
Winter (Dec.-Feb.)	16.32	12.76	6.38	11.35	

a: 0.5 PV-only; b: 0.4 PV-0.1Wind; c: 0.4 PV-0.1Wind-2.5h Storage@ 0.25 max. power capacity; d: 0.3 PV-0.2 Wind;

Interestingly, for the summer season increasing the wind capacity/share of the hybrid system (as found with PV-W2 system), the percentage peak load reduction is seen to

rather drop in magnitude (from 5.59% to 4.82%; see columns 3 and 5) as compared to the PV-W1 system.

This contrast with the other seasons is somehow expected in warm climates since the monthly cumulative wind power output is normally found to be at its lowest in the summer season as opposed to solar power. Thus, reducing the PV share in favor of wind capacity could invariably reduce the aggregate summer output. Moreover, referring to Table 3.2 (in chapter 3) the wind power for the area under consideration was found to anti-correlate with the grid load, the strongest seen in summer. This also offers some explanation to the lesser impact of the PV-W2 system in reducing the summer peak.

The storage integrated hybrid system (i.e. PV-W1-S) is seen not having any appreciable impacts on both the peak load reduction and energy penetration during the summer season. An insight to the reason for this could be seen from a plot of the net daily stored energy of the storage system showing the summer season. Figures 4.6 and 4.7 present the net daily and hourly storage energy capacities for the PV-W1-S hybrid system during the year.

From Figure 4.6 it is seen that during the summer period (from the 152th to the 243th day of the year), which also represents the grid annual peak demand period, all the available storage capacities if they exist, are used up during the day. Figure 4.7 further reveals that apart from the early weeks of summer (i.e. 3625~3950 hours), the storage does not even receive any boost for the rest of the defined summer period, indicating no excess renewable generation.
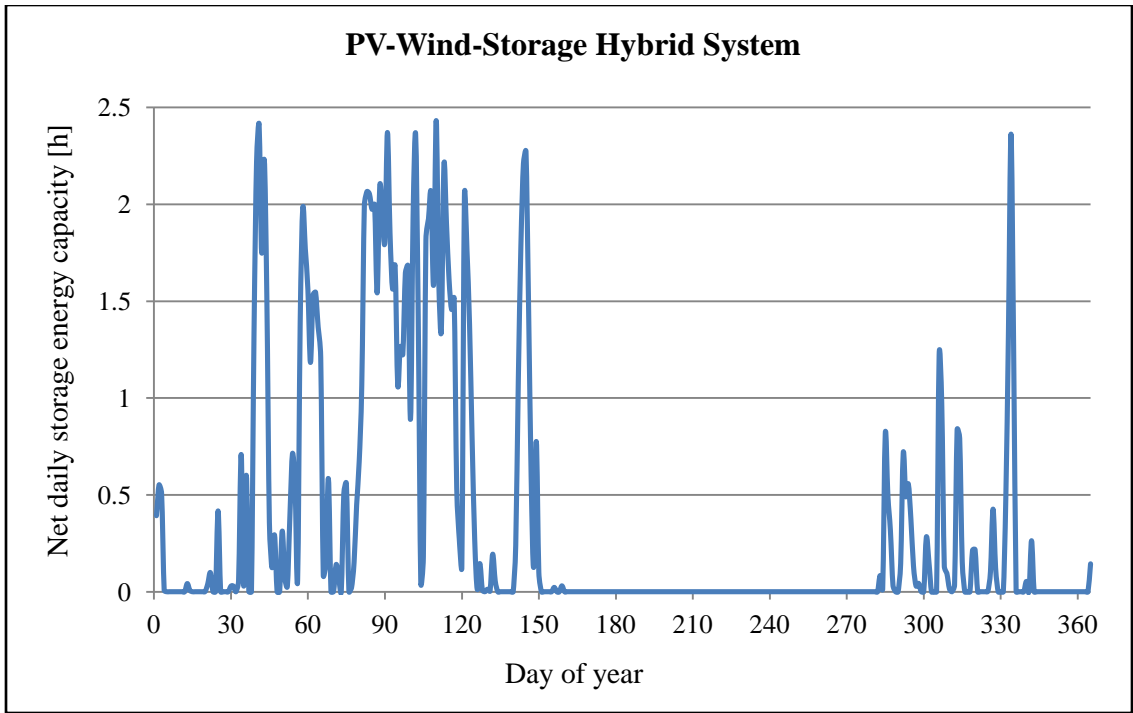
Figure 4.6: Net daily storage energy capacities for PV-W1-S system
(PV = 0.4; wind = 0.1; max. storage caps. [power = 0.25, energy = 0.5]; base gen. = 0.28)
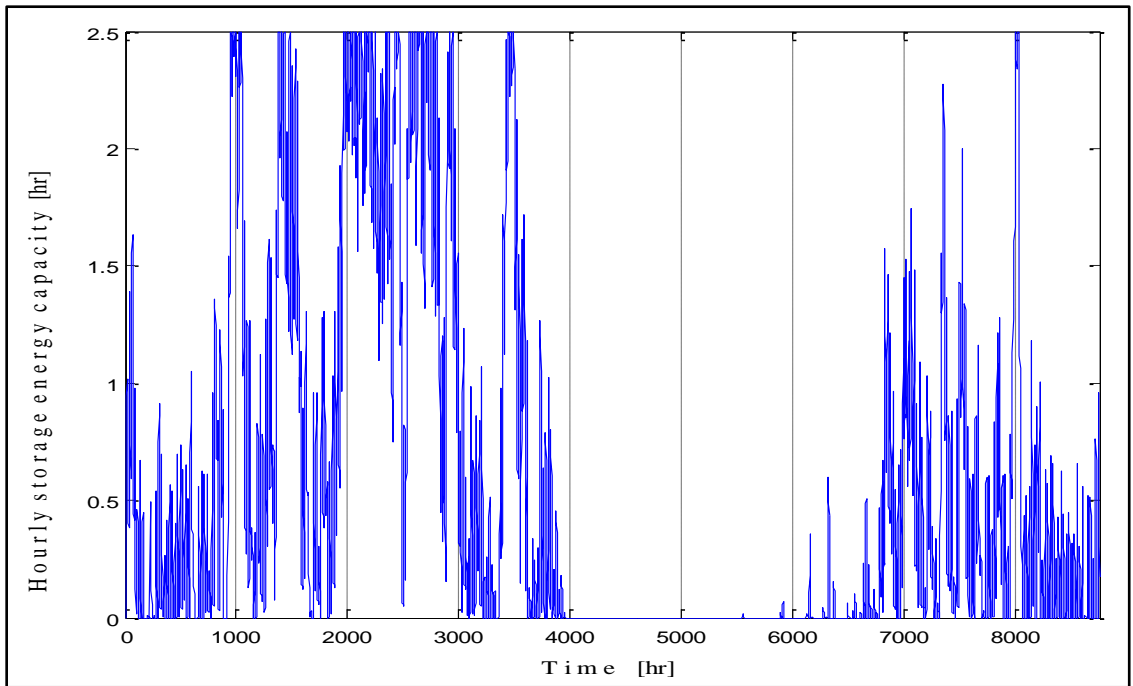
Figure 4.7: Hourly storage energy capacities for PV-W1-S system

54

Moreover, the closeness of summer season's energy penetrations for both PV-W1 and PV-W1-S systems (Table 4.2) is due to the fact that the aggregate renewable energy generation fits relatively well with the season's demand pattern/profile. As a result there is practically no excess renewable generation available as indicated by Figures 4.6 and 4.7, and as will be seen later from Figure 4.10.

4.4.2 Storage discharge strategy for load leveling or peak shaving

The preceding analysis for sizing the storage size assumed a parallel stock and flow process. In others words, the storage is made available on the grid as part of the grid energy supply capacity throughout the day. It is discharged when supply deficit requires, nonetheless, should have available capacity and be charged when there is excess renewable generation on the grid. However, for utilities the practical storage dispatch approach for load leveling (or peak shaving) would be to store up energy during off-peak times of the day and use during peak times. This stems from the fact that oftentimes energy is mostly available and the cost is cheaper during off-peak times as opposed to on-peak times.

Before comparisons are made of the impact of the hybrid systems on the daily peak load (as covered in the next section, 4.4.3), the season's daily on-peak period(s) would be assumed and fixed as follows where the energy storage is put on line.

- Spring season : 11am – 5pm
- Summer season: 11am – 7pm
- Fall season : 11am – 5pm
- Winter season: 11am – 5pm

Moreover, a novel conception about the storage dispatch (being referred to as *StorageShare_peak*) for this analysis was the assumption that the available storage energy capacity during peak period is discharged (if required) in equal amounts between the present hour of peak period and the end of the peak period. Thus, the available energy capacity for discharge during any hour of the peak period could be thought of as some kind of a moving average. The mathematical description is given in Eq.(4.1) following as:

$$StorageShare_{peak} = \frac{Capacity_{t-1} - Capacity_{min}}{t_{peak_{end}} - t_j + 1} \qquad (4.1)$$

where

- *Capacity$_{t-1}$* is the available energy capacity preceding the present peak hour
- *Capacity$_{min}$* is the minimum capacity to which the storage can be discharged
- *t$_{peak\_end}$* is the end hour of the peak period
- *t$_j$* is the present peak hour

The objective of this dispatch methodology is to avoid the possibility of the storage being depleted before the peak period was over, and as such to have the storage available to back up the renewable output during such 'critical' period. Do refer to Appendix for more details.

During off-peak period the priority of the renewable generation would be to charge the storage and when its full energy capacity is achieved then the remaining renewable generation is put onto the grid, however, limited by the base generation. The reverse applies during peak times. However, this strategy could possible add to the losses of renewable generation because of the charging and discharge inefficiencies of the energy storage system. This would be ascertained from the next section of the analysis.

4.4.3 Daily peaks

In this section plots of a 7-day (Monday through Sunday) grid net load profile for selected months of the seasons are presented. The purpose of doing this is to depict typical seasonal weekly load patterns that compare the PV-W1 hybrid system and the PV-W1-S (i.e. with integrated energy storage) hybrid system. These are shown in Figures 4.8 through 4.11. Note that this analysis is carried out assuming constant base generation of 0.28.

From the Figures 4.8 to 4.11 it is seen that except for the selected week in April (of the spring season) the grid load/demand is generally reduced during weekends. This observation is expected since typically there is less power demand from most commercial buildings (offices, industrial machinery and others) in this time period.

Looking at Figure 4.10, the renewable energy generations for both hybrid systems are seen to fit quite well with the grid demand profile. Consequently they are both found to supply the July (summer) peak demand hours very well, reducing and shifting the observed daily peak loads to about 3 and 4 hours later (typically from 4pm to 7pm and 8pm) during weekdays for the PV-W1 system and the PV-W1-S system respectively. Actually, the selected week contains the annual peak load which was recorded on the 4th day (@ 88th week hour or 4pm on Thursday).

Referring to Figure 4.11, for the week of October (fall season) the generation profiles from both systems are found to slightly match the demand profile. The hybrid systems are seen to reduce the peak loads by some few percentage points as well as narrowing the peak demand hours. For the other selected weeks of January (winter) and April (spring) the RE generations are found to be less coincident with the peak demand hours.
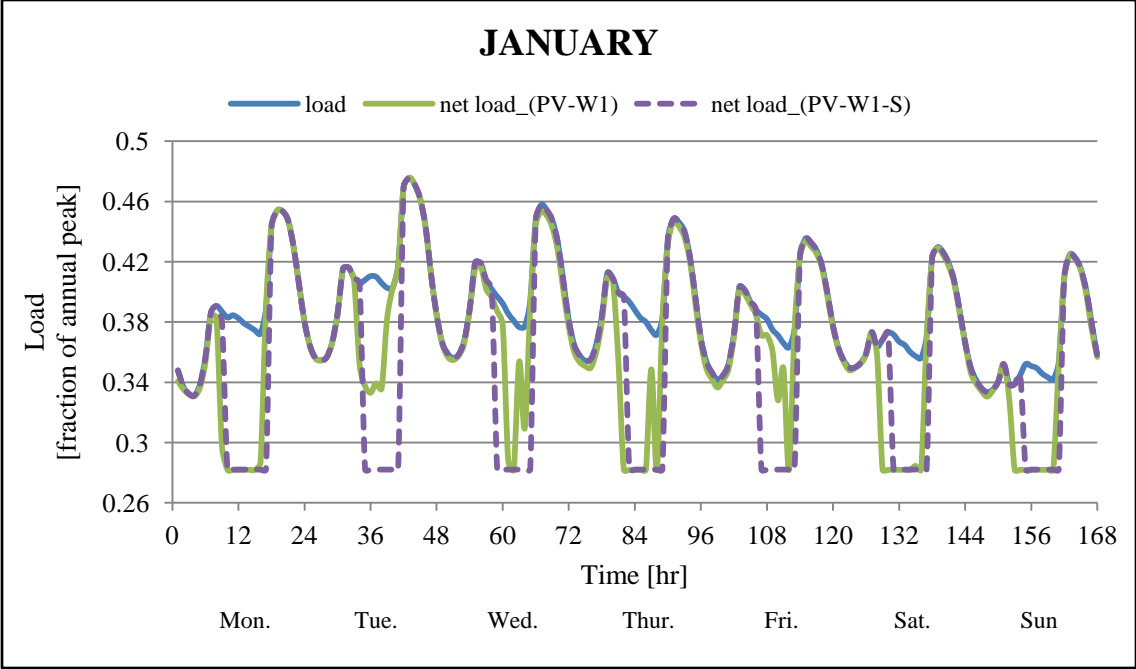
Figure 4.8: Comparison of daily net load patterns in a week of January (7th − 13th)
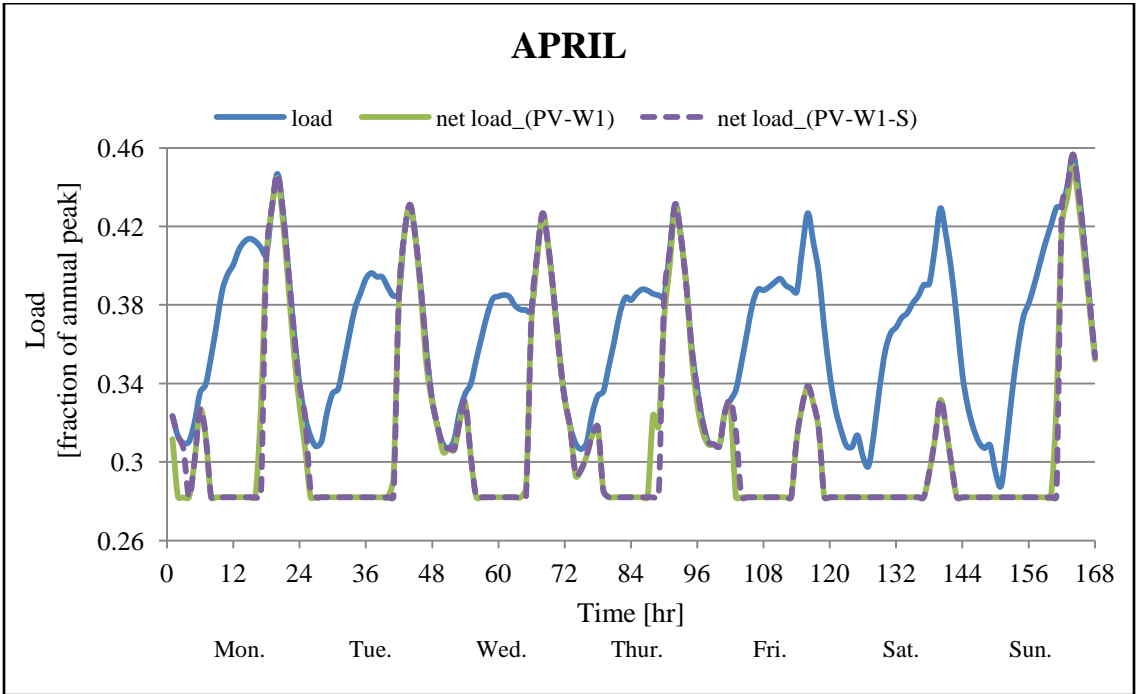
Figure 4.9: Comparison of daily net load patterns in a week of April (7th − 13th)

58
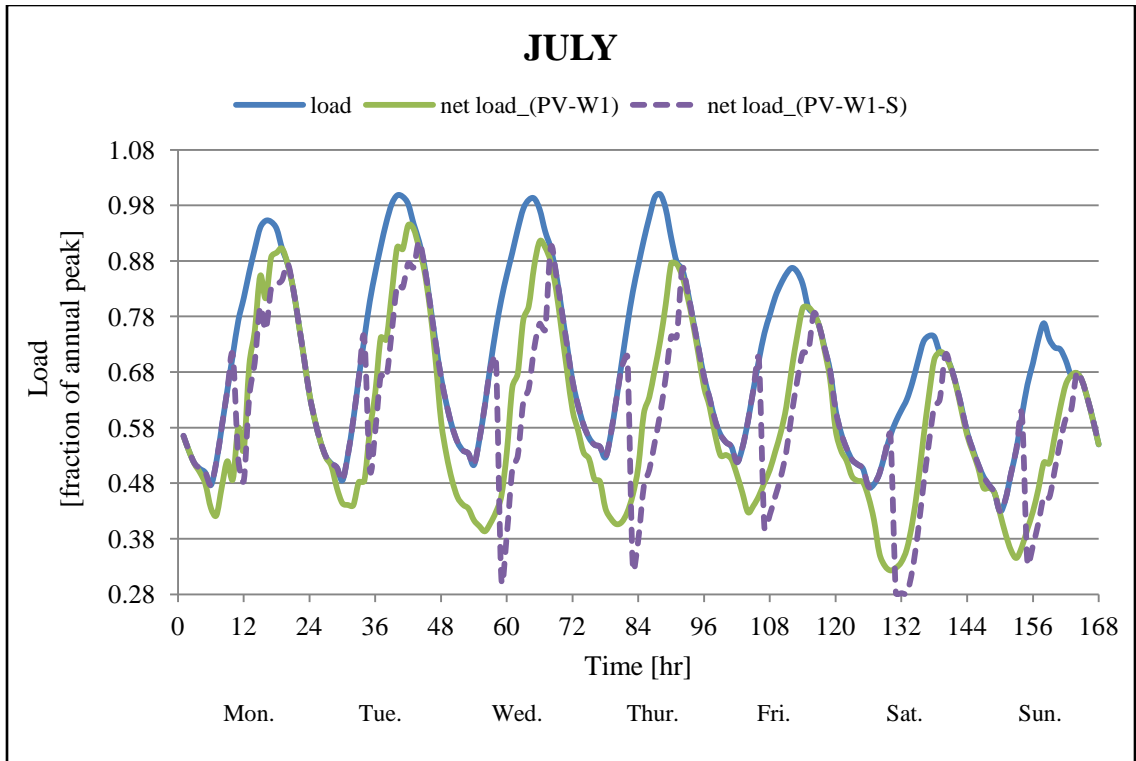
Figure 4.10: Comparison of daily net load patterns in a week of July (7th – 13th)
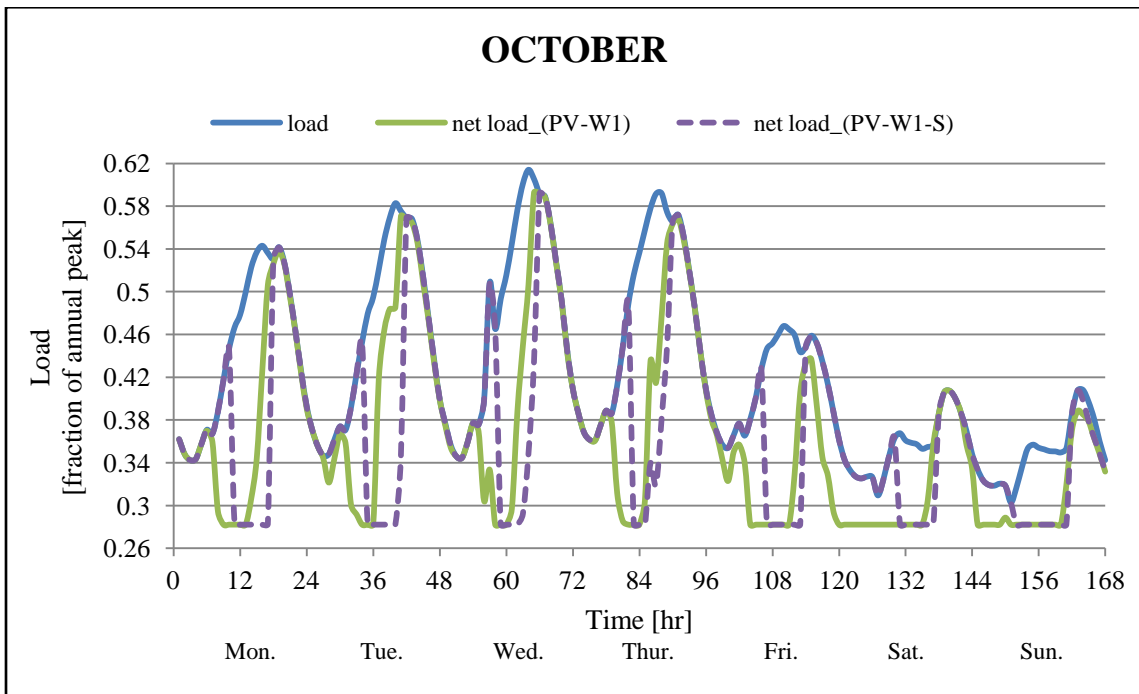
Figure 4.11: Comparison of daily net load patterns in a week of October (6th – 12th)

59

However, considering the spring season, both systems are observed to impact very well on the first peak period (refer to Figure 4.9) by supplying all the required grid demand. Generally both the wind and the PV outputs assume higher output values during the spring season and as such leading to their ability to deal with the morning to late afternoon demand and even left with excess generation for storage charging as had already been seen and discussed in the preceding sections.

To further compare the performance of the PV-W1 and PV-W1-S hybrid systems, the following energy-based performance metrics were adopted for the analysis. They are the: energy penetration, peak load reduction, system energy loss and grid supply deficit all evaluated on annual basis. The performance characteristics values obtained for both systems are presented in Table 4.3.

Table 4.3: Energy performance characteristics for the PV-W1 and PV-W1-S hybrid systems

Parameter	PV-W1	PV-W1-S	Notes
Energy penetration	15.34	14.85	% of total grid demand
Peak load reduction	5.59	8.54	% of annual peak load
System energy loss	27.30	29.11	% of total renewable generation
Supply deficit	8.75	5.52	% of total grid demand

From Table 4.3 it is realized that the non-storage integrated system out performs the storage-integrated system in terms of annual renewable energy penetration. Recall from section 4.4.2 (in the last paragraph) it was said the storage dispatch strategy being adopted could possible increase the system energy losses because of the charging and discharge inefficiencies of the energy storage system. Thus any chance of using the

output from the renewable generation directly is always desired at least from the standpoint of efficient utilization. This explains the higher value of the energy penetration for PV-W1 system over the PV-W1-S hybrid system. Actually about 4% of the PV-W1-S system total energy loss is coming from the storage system. However, the benefit of the storage integrated system (i.e. PV-W1-S) is seen the area of the annual peak load reduction which is about three (3) percentage points over that of the corresponding non-integrated storage hybrid system.

4.5 Seasonal optimal mix between wind and solar (PV) power generations

In this section the results of the search for an energy-based optimal combination of solar (PV) and wind power for a hypothetical 100% renewable grid supply generation is presented. The diurnal and seasonal patterns of the solar and wind power generations are evaluated.

4.5.1 Annual diurnal variation of the load, solar and wind

One of the ways to compare and correlate the wind and solar power potentials for supplying the given load profile is to examine their diurnal patterns. Figure 4.12 presents the annual average diurnal patterns of the load, solar and wind power generations.
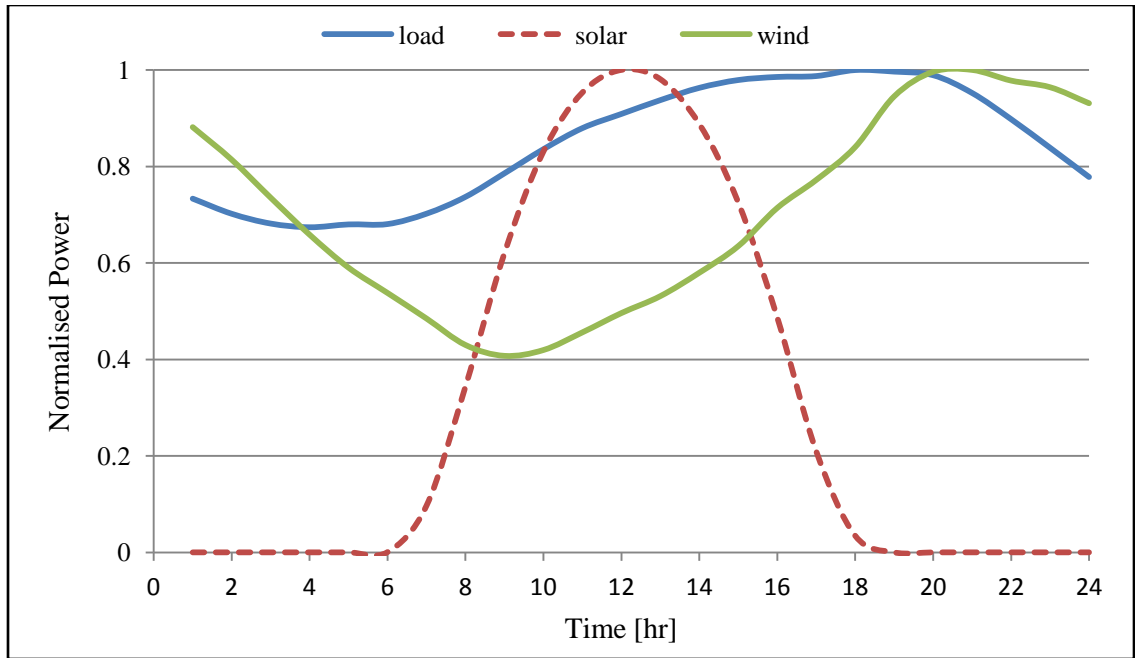
Figure 4.12: Annual average diurnal patterns of the load, solar (PV) and wind power

From Figure 4.12, as expected the solar PV generation picks up in the morning, peaks at mid-day, and sets between 18:00 and 19:00 hours of the day. The wind generation on the other hand has its peak values in the night, continues on the downward trend till late morning and then picks up again. In Figure 4.12 the desired complementary outputs of the wind and solar power are observed not to be strong. This confirms the evaluated smaller value for the correlation coefficient obtained in Table 3.2 and the statement made towards it, that wind and solar might not complement well to serving the grid load for the geographical area under consideration. This observed pattern could lead to a disproportionate fraction in favor of solar PV in an attempt to find the seasonal optimal combination of the two resources for 100% grid supply scenario.

4.5.2 Seasonal variation of the load, solar and wind generations

Having examined the annual average diurnal patterns, the seasonal variations are then evaluated. Figure 4.13 presents the seasonal/monthly variations of the load, solar (PV) and wind power generations.
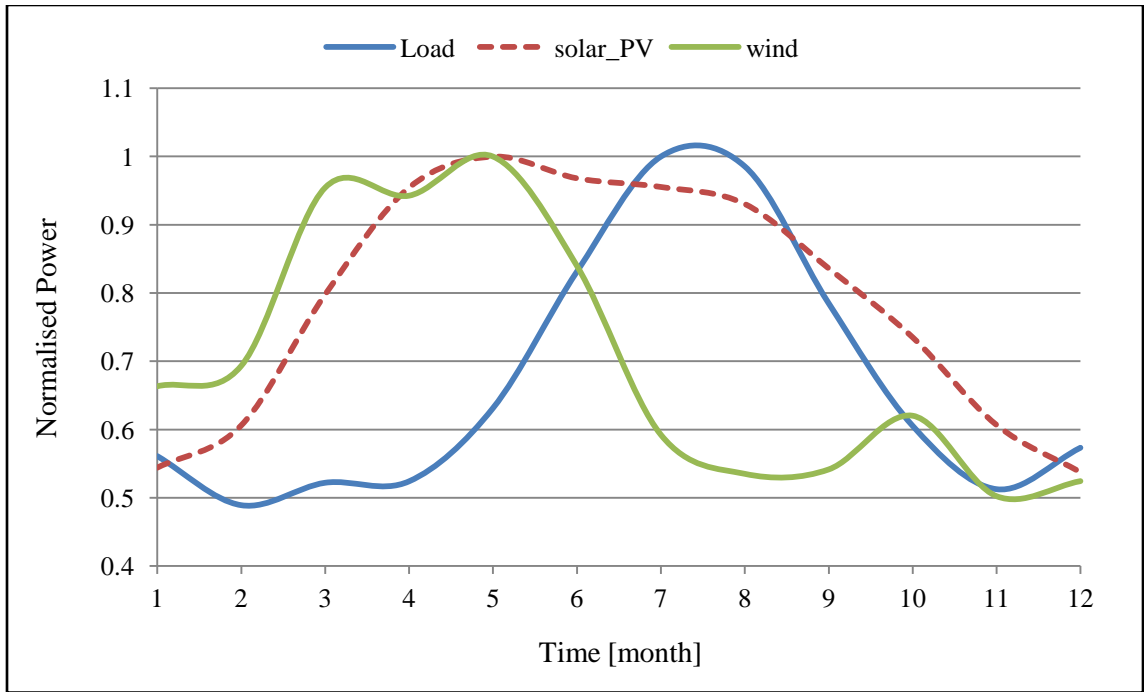
Figure 4.13: Seasonal average patterns of the load, solar PV and wind power generations

From Figure 4.13 it is observed that the inference drawn from Figure 3.12 and Table 3.2 about the non-complementary nature of the wind and solar (PV) generations in the geographical area under consideration is confirmed. Both the wind and solar PV power have their peak or close to peak generations in the spring season (March – May) and with the wind dropping to its lower values in summer. Moreover, though the solar radiation is generally high in summer season, one can see from the plot (Figure 4.13) that the solar

PV energy output rather reduces a bit compared with the output in May (in a spring season month). This can be attributed to the sensitivity of silicon cells to high ambient temperatures, and thus having reduction in their performance at those summer elevated temperatures.

The patterns observed for the two generations do not readily serve as an attraction for combining them with the aim of grid peak load/demand reductions and the futuristic objective of 100% wind-solar grid supply generation. As aforementioned, this would tilt the scale much in favor of the solar PV in any attempt to find the seasonal optimal mix. It will be confirmed in the next section.

4.5.3 Seasonal optimal combination/weighting of solar and wind generations

Figure 4.14 shows the result of the load matching profile of the seasonal optimal combination of solar PV and wind power generations based on minimum summer season energy deficit. Executing the algorithm for the evaluation of the seasonal optimal combination of the solar PV and wind power generations, it was found that to match the given grid load profile and with a maximum supply generation to the summer load, it will require that 95% of grid load has to be supply with the solar PV generation whereas the wind takes the remaining 5%. The required installed capacities could be derived from this by multiplying the respective percentages by the total grid load to obtain the resulting annual total generation requirements. With these values one can then determine either the PV or wind installed capacity required to output that annual total energy value.
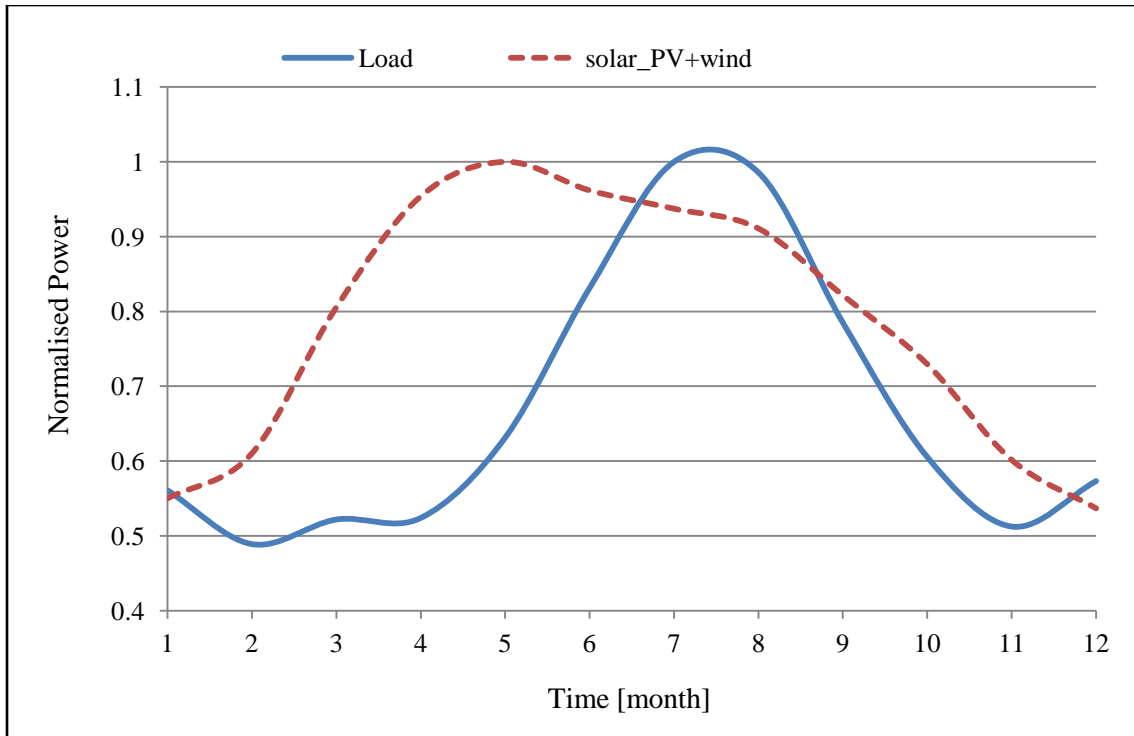
Figure 4.14: Optimal seasonal weighting of 95%/5% (solar/wind) generation requirement

From Figure 4.14 it seen that even with this optimal mix there will be enormous excess generation in the spring season (March – May) and also during the fall season (August – November). These large surpluses do not represent economic use of infrastructure, and can be more beneficial if some sort of storage is employed. Also, the use of conventional plant(s) as backups could help with making up for the summer generation deficit.

CHAPTER 5

CONCLUSIONS AND RECOMMENDATIONS

Renewables will continue to be inherently intermittent. However, to smooth out this variability and enhance their desirability for utility scale deployment in electric power systems, some form of buffering system and hence supplemental energy storage will be required. Moreover, the seemingly natural complementing profiles of wind and solar resources provide an opportunity for dealing with their variability and as such for their exploitation for electricity production.

In this work a MATLAB code has been developed which helps to provide preliminary estimates of maximum required annual energy storage capacities for a given grid load data/profile. Energy storage cycle (i.e. round-trip) efficiency of 80% and inherent/self discharge losses of 10% of available capacity per month were assumed for the analysis.

By allowing for about 7.5% loss (i.e. dumped + storage charging and discharging losses) of annual PV energy output, the energy-based optimized storage capacity was found as (power = 0.25, energy = 2.5 h) and resulting in annual energy penetration of 17.86% for 0.5 PV size and 0.28 base generation capacity. This contrasts the non-dumped storage capacity (power = 0.31, energy = 11.04; refer Table 4.1) observed for the same configuration, however, with storage system losses of 6.4% of annual PV output and annual energy penetration of 18.06%.

Thus, it is noted that sizing of the required storage capacities based on losses resulting only from cycle efficiency and self-discharge losses could potentially lead to a 'wasteful'

sizing. In practice, settling on the optimum size of annual required storage capacity will be made based upon factors inclusive of the operating strategies to be employed and percentage of other energy losses to be accepted.

The deployment of greater capacities of either wind or solar PV power on the current grid for the study area poses challenge for utilities to seek bigger energy storage capacities for storing the excess generation (especially in the spring season) if no dumping is considered. Otherwise, there must be other strategies to deal with the excesses.

Performance analysis and comparisons of non-storage and storage-integrated hybrid systems (using PV-W1 and PV-W1-S) have been carried out. The following energy based performance metrics - energy penetration, peak load reduction, system energy loss and grid supply deficit - all on annual basis were adopted (refer Table 4.3). For the analysis, the deployment of the energy storage for complementing the supply generation was considered only during defined peak period whereas it was charged with only the renewable generations during off-peak period. Such deployment is thought to closely resemble the practical use of storage by utilities for peak load shaving/leveling.

The complementary nature observed for solar PV and wind power generation profiles for the study area were found to be weak on seasonal basis (see Figure 4.13). Thus the two resources/generations do not readily serve as an attraction for deploying them in tandem to effectively match the seasonal grid demand in the futuristic objective of 100% wind-solar grid supply generation. Consequently, a seasonal optimal mix weighting of 95%/5% in favor of solar PV for meeting the given grid load profile and based on minimum summer supply deficit, was observed for their combination. However, be

advised that this evaluation applies only to the study area (which is southern Nevada) and could significantly change when an area with good wind resource is considered. The above analysis though evaluated for non-tracking solar PV system is presumed to follow similar patterns when considered for other solar PV technologies and tracking strategies.

It is noted here that one significant limitation or challenge to this study was the acquisition of utility hourly load data. It is recommended for further work that:

- load data that extends a couple of years be acquired for such analysis to help 'truly' examine the average seasonal and or diurnal load patterns and make the results/conclusions more encompassing;

- such analysis be performed on a finer time scales/steps of less than one (1) hour to evaluate the interactions among the hybrid system components (solar-wind-energy storage), which may give additional insight to the storage needs;

- some sort of economic evaluations be incorporated.

APPENDIX

Hybrid Electric Power System Model with MATLAB

```
%SIMULATION OF HYBRID (solar+wind+storage)ELECTRIC POWER SYSTEMS.
%
clear all
clc
tic  %to check run/simulation time
%
%
%%%%%%%%%%%%%%%%%%%%%%%%%%%%
%INPUT
%%%%%%%%%%%%%%%%%%%%%%%%%%%%
%
%%%%Import hourly power data/values from excel
%-------------------------------------------------------------------
%NOTE:-ALL hourly values are normalized to the annual peak hourly grid load
Data = xlsread('ThesisData_In',2,'B3:E8762');
%
Time = Data(:,1);
Load_1 = Data(:,2);             %Grid demand/load
Solar_1 = Data(:,3);            %PV output
Wind_1 = Data(:,4);             %Wind energy output
%
MaxLoad = max(Load_1);
MaxPV = max(Solar_1);
MaxWnd = max(Wind_1);
%
%Base Generation
BaseGenVar = 0;         %set to zero (0) for constant annual base gen
                        %set to 1 for seasonal base gen
%....if assumed annual constant
BaseGen_Annual = min(Load_1);
%....if assumed seasonal variable
Winter1 = min(Load_1(1:24*59));
Winter2 = min(Load_1(24*334+1:24*365));
BaseGen_Winter = min(Winter1,Winter2);          %Dec-Feb
BaseGen_Spring = min(Load_1(24*59+1:151*24));    %Mar-May
BaseGen_Summer = min(Load_1(24*151+1:243*24));   %Jun-Aug
BaseGen_Fall = min(Load_1(24*243+1:24*334));     %Sep-Nov
%
%
%%%%Scaling of capacities (output) of hybrid plants
%-------------------------------------------------------------------
f_slr = 4;                      %solar pv [1 is equiv. to 10% of peak load]
f_wnd = 1;                      %wind
%
%
%%%%Storage Characteristics
%-------------------------------------------------------------------
eff_cycle = 0.8;        %cycle/round trip efficiency
eff_c = sqrt(eff_cycle);  %charging efficiency(assumed same as discharge)
eff_d = sqrt(eff_cycle);  %discharging efficiency
selfdschg = 1.39*10^-4;   %self-discharge per hour [assumed 10% per month
%                              ...of available capacity]
%
```

```matlab
H_t_max = 0.25*MaxLoad;     %maximum discharging/charging power capacity
dschgTime =10;              %[hr]storage discharge time @ max power capacity
H_max = dschgTime*H_t_max;     %max storage energy capacity
H_min = 0*H_max;            %assumed min storage energy capacity
%
%Initialization of other parameters
%-----------------------------------------------------------------------
H_old =H_min;            %storage energy level or capacity at time t=0 or(t-1)
Ebse_dump = 0;             %base generation dumped
hr_bd = 0;                 %hours of dumping of base generation
offpk_hrs =0;              %off-peak hours
onpk_hrs=0;               %on-peak hours
%
BaseGenVar =0;         %Apply variable/seasonal base gen. yes=1 and no=0
PkDmdApp=0;      %set to 1 to apply peak and off peak; otherwise set to zero
dmf_red_applied = 1;   %applying demand-following reduction strategy during
%                      ...off peak; yes=1 and no=0
StrShare_Pk =0;
%
%%%%%%%%%%%%%%%%%%%%%%%%%%%%%%%%%%%%%%%%%%%%%%%%%%%%%%%%%%%%%%%%%%
%CALCULATIONS (Dispatch strategy for the PV/Wind/Storage system)
%%%%%%%%%%%%%%%%%%%%%%%%%%%%%%%%%%%%%%%%%%%%%%%%%%%%%%%%%%%%%%%%%%
%-----------------------------------------------------------------------
 for i=152:243                      %day of year
   %
   if PkDmdApp ==0
      peak1_start = 0;
      peak1_end = 24;
      peak2_start = peak1_start;
      peak2_end = peak1_end;
   else
   %....setting of the demand periods (peak and off-peak)
    if i>59 && i<=151              %spring
      peak1_start = 11;           %hour beginning the peak period
      peak1_end = 17;             %hour ending the peak period
      peak2_start = peak1_start;
      peak2_end = peak1_end;
    elseif i>151 && i<=243        %summer
      peak1_start = 11;
      peak1_end = 19;
      peak2_start = peak1_start;
      peak2_end = peak1_end;
    elseif i>243 && i<=334        %fall
      peak1_start = 11;
      peak1_end = 17;
      peak2_start = peak1_start;
      peak2_end = peak1_end;
    else                          %winter
      peak1_start = 11;
      peak1_end = 17;
      peak2_start = peak1_start;
      peak2_end = peak1_end;
    end
   %
   end
      %
   if BaseGenVar == 0
      %...if considering annual constant base gen
      f_bse = BaseGen_Annual;
   else
```

```matlab
   %...if considering variable/seasonal base gen
 if i>59 && i<=151
    f_bse =BaseGen_Spring;
 elseif i>151 && i<=243
    f_bse =BaseGen_Summer;
 elseif i>243 && i<=334
    f_bse =BaseGen_Fall;
 else
    f_bse =BaseGen_Winter;
 end
  %
end
%
  for j=1:24                 %hour of day
     k = 24*(i-1)+j;         %hour of year
     %
     Load(i,j) = Load_1(k,1);         %just for reformatting the data
     Solar(i,j) = Solar_1(k,1);       %         -do-
     Wind(i,j) = Wind_1(k,1);         %         -do-
     %
     Eout_pv(i,j) = f_slr*Solar(i,j);     %scaled hourly solar output
    Eout_w(i,j) = f_wnd*Wind(i,j);        %scaled hourly wind output
    Eout_RE(i,j) = f_slr*Solar(i,j)+f_wnd*Wind(i,j);%Total ren. Gen.
    %+++++++++++++++++++++++++++++++++++++++++++++++++
   %%OFF PEAK hours [assumed demand met with other plants exclusive of
    %              ...PV/Wind/Storage]
    %+++++++++++++++++++++++++++++++++++++++++++++++++
    if (j<peak1_start || j>peak1_end)&&(j<peak2_start || j>peak2_end)
         DsgLoss(i,j)=0;               %storage discharging energy loss
         Eout_dmf_OnPk(i,j) = 0;     %demand following generation for
         %                      ...ON PEAK period
         Eout_dmf_OnPk_str(i,j) = 0;
         offpk_hrs=offpk_hrs+1;
         Eout_bse(i,j) = f_bse*MaxLoad;        %base generation
         E_mb(i,j) = Load(i,j)-Eout_bse(i,j);   %mismatch energy after
         %                      ...considering only base generation
         if E_mb(i,j)==0
            Eout_dmf_OffPk(i,j)=0;          %for non-storage system
            Eout_dmf_OffPk_str(i,j) = E_mb(i,j); %initial assumption,
         % ...because charging of storage is priority during OFF PEAK
            Edump_RE(i,j) = Eout_RE(i,j)     %i.e. demand is met, and
            %                      ...excess gen. from RE is dumped
         elseif E_mb(i,j)>0        %i.e. deficit in supply generation
            %RE only system (i.e. non-storage system)
          Eout_dmf_OffPk(i,j)=E_mb(i,j)-Eout_RE(i,j);%for RE only sys
          Edump_RE(i,j) = 0;
            if Eout_dmf_OffPk(i,j)<0  %more RE gen. than demanded
               Edump_RE(i,j) = abs(Eout_dmf_OffPk(i,j));
               Eout_dmf_OffPk(i,j)=0;
            end
          Eout_dmf_OffPk_str(i,j) = E_mb(i,j);  %because charging of
          %                     ...storage is priority during off peak
         else  %not demanded if all times Load(i,j)>=Eout_bse(i,j);
            Ebse_dump = Ebse_dump + abs(E_mb(i,j));
            hr_bsd = hr_bsd + 1;        %hours of dumping of base gen
            Eout_dmf_OffPk(i,j)=0;
            Eout_dmf_OffPk_str(i,j)=0;
            Edump_RE(i,j) = Eout_RE(i,j);
         end
         Load_net(i,j) = 0;     %hour grid demand is fully met i.e no
```

71

```matlab
%                        ...residual load
Load_net_str(i,j) = 0;  %-do- (for integrated str. scenario)
Eout_deficit(i,j) = Load_net(i,j);
Eout_deficit_str(i,j) = Load_net_str(i,j);
%
%RE generation during off peak
E_ms(i,j)= Eout_RE(i,j); %mismatch energy (=gross RE output)
%
%charging of storage with RE generation
H_t(i,j) = eff_c*E_ms(i,j);    %actual energy to charge str.
ChgDsgLoss(i,j) = (1-eff_c)*E_ms(i,j);  %loss due to storage
%                        ...charging or discharging
ChgLoss(i,j) = (1-eff_c)*E_ms(i,j);
Edump_RE_str(i,j)= 0;
Eusable_RE_str(i,j)=0; %=0 since not contributing to the load
%                        ...immediately
%
if H_t(i,j)>H_t_max  %i.e. if the required power cap. @ time
 %                   ...t is greater than the str. max pwr cap
   H_t(i,j)=H_t_max;
  Edump_RE_str(i,j) = E_ms(i,j)-(H_t(i,j)/eff_c); %excess RE
   %              ...generation w.r.t str charging is dumped
   ChgDsgLoss(i,j) = (1-eff_c)*(H_t(i,j)/eff_c);
   ChgLoss(i,j) = (1-eff_c)*(H_t(i,j)/eff_c);
   Eusable_RE_str(i,j) =0;
   %....if surplus RE generation is used to reduce required
   %                        ...demand-following generation
      if dmf_red_applied == 1
        Eout_dmf_OffPk_str(i,j)=E_mb(i,j)-Edump_RE_str(i,j);
         Eusable_RE_str(i,j) = Epv_dump_str(i,j);
         Edump_RE_str(i,j)=0;
         if Eout_dmf_OffPk_str(i,j)<0
            Edump_RE_str(i,j)=abs(Eout_dmf_OffPk_str(i,j));
            Eusable_RE_str(i,j) =E_mb(i,j);
            Eout_dmf_OffPk_str(i,j)=0;
         end
      end
end
H_new = H_old+H_t(i,j);
%
  if H_new>H_max     %i.e. if max energy storage capacity is
     %                                   ...surpassed
     H_t(i,j) = H_max-H_old;
%NOTE:if it is assumed for now that all surplus RE after str
   %                                   ...charging is dumped
     Edump_RE_str(i,j) = E_ms(i,j)-(H_t(i,j)/eff_c);
     ChgLoss(i,j) = (1-eff_c)*(H_t(i,j)/eff_c);
     ChgDsgLoss(i,j) = (1-eff_c)*(H_t(i,j)/eff_c);
     Eusable_RE_str(i,j) = 0;
   %**if surplus RE generation is used to reduce required
   %                        ...demand-following generation
     if dmf_red_applied == 1
        Eout_dmf_OffPk_str(i,j)=E_mb(i,j)-Edump_RE_str(i,j);
        Eusable_RE_str(i,j) = Edump_RE_str(i,j);
        Edump_RE_str(i,j)=0;
        if Eout_dmf_OffPk_str(i,j)<0
           Edump_RE_str(i,j)=abs(Eout_dmf_OffPk_str(i,j));
           Eusable_RE_str(i,j) = E_mb(i,j);
           Eout_dmf_OffPk_str(i,j)=0;
        end
```

```
                        end
                        H_new=H_max;
                    end
    %+++++++++++++++++++++++++++++++++++++++++++++++++++++++++++++++++
    %ON peak hours [Storage system contributes to grid supply]
    %+++++++++++++++++++++++++++++++++++++++++++++++++++++++++++++++++
     else
        ChgLoss(i,j)=0;              %initial assumption of no charging
        Eout_dmf_OffPk(i,j)= 0;   %demand following generation (OFF PEAK)
        Eout_dmf_OffPk_str(i,j)= 0;
        onpk_hrs = onpk_hrs+1;
        Eout_bse(i,j) = f_bse*MaxLoad;      %base generation
        E_mb(i,j) = Load(i,j)-Eout_bse(i,j);    %mismatch/residual load
        %                         ... after accounting for only base gen.
            %
            if E_mb(i,j)>=0
                E_ms(i,j) = Eout_RE(i,j)-E_mb(i,j);    %mismatch load after
                %            ...accounting for both RE and base generation
            else
             %..(not needed if min. load is considered for the base gen.)
                Ebse_dump = Ebse_dump + abs(E_mb(i,j)); %dumped base energy
             %...(not needed if we consider no dumping for base generation
                hr_bsd = hr_bsd + 1;             %hours of dumping base gen
                E_ms(i,j) = Eout_RE(i,j);
            end
             %
             if E_ms(i,j)>=0   %i.e. having equal/excess supply (i.e. RE)
             %                                    ...over net grid demand
                Eout_dmf_OnPk(i,j)= 0;   %i.e. no demand following gen.
                 Eout_dmf_OnPk_str(i,j)= 0;
                 %
                 %for non-storage scenario
                  Edump_RE(i,j)= E_ms(i,j);
                  Eout_deficit(i,j)=0;         %i.e no residual grid load
                  Load_net(i,j) = Eout_deficit(i,j);
                 %
                 %for storage integrated scenario
                 Eusable_RE_str(i,j) = E_mb(i,j); %actual RE gen. used to
                 %                ...service demand; rest go into storage
                  Eout_deficit_str(i,j)=0;
                  Load_net_str(i,j) = Eout_deficit_str(i,j);
                  %....charge storage with excess RE gen.
                  H_t(i,j) = eff_c*E_ms(i,j);
                  Edump_RE_str(i,j) = 0; %initial assumption that all the
                  %                  ...charging supply will go into str.
                  ChgDsgLoss(i,j) = (1-eff_c)*E_ms(i,j);
                  ChgLoss(i,j) = (1-eff_c)*E_ms(i,j);
                  %
                  %...charging storage in consideration of power capacity
                  if H_t(i,j)>H_t_max
                     H_t(i,j)=H_t_max;
                     Edump_RE_str(i,j) = E_ms(i,j)-(H_t(i,j)/eff_c);
                     ChgDsgLoss(i,j) = (1-eff_c)*(H_t(i,j)/eff_c);
                     ChgLoss(i,j) = (1-eff_c)*(H_t(i,j)/eff_c);
                     Eusable_RE_str(i,j) = E_mb(i,j);
                  end
                    H_new = H_old + H_t(i,j);
                    %
                    %..charging of storage with regard to max. energy cap.
                     if H_new>H_max  % max str. energy cap.is surpassed?
```

```matlab
                        H_t(i,j) = H_max-H_old;
                        Edump_RE_str(i,j) = E_ms(i,j)-(H_t(i,j)/eff_c);
                        ChgDsgLoss(i,j) = (1-eff_c)*(H_t(i,j)/eff_c);
                        ChgLoss(i,j) = (1-eff_c)*(H_t(i,j)/eff_c);
                        Eusable_RE_str(i,j) = E_mb(i,j);
                        H_new=H_max;
                    end
            %

%%%%%%%%%%%%%%%%%%%%%%%%%%%%%%%%%%%%%%%%%%%%%%%%%%%%%%%%%%%%%%%%%%%%%%%%
            %....discharging from storage because of supply deficit
            elseif E_ms(i,j)<0
                    % for non-storage case
                    Edump_RE(i,j)=0;
                    Load_net(i,j) = abs(E_ms(i,j));
                    Eout_deficit(i,j) = Load_net(i,j);
                    Eout_dmf_OnPk(i,j)= abs(E_ms(i,j));
                    %
                    % for storage integrated system case
                    if j<peak2_start
                        peak_end = peak1_end;
                    elseif j>=peak2_start
                        peak_end = peak2_end;
                    else
                    end
                    StrShare_Pk = (H_old-H_min)/(peak_end-j+1);
                    Edump_RE_str(i,j)=0;
                    H_t(i,j) = abs((E_ms(i,j)/eff_d));    %discharge energy
        %..from storage (incl. losses)to make up for the remaining load
                    %
                    %..if there is sufficient str. cap. to meet demand
                     if H_t(i,j)<= StrShare_Pk
                        Load_net_str(i,j) = 0;
                        ChgDsgLoss(i,j)=(1-eff_d)*H_t(i,j);
                        DsgLoss(i,j)=(1-eff_d)*H_t(i,j);
                        Eout_deficit_str(i,j) = Load_net_str(i,j);
                        Eout_dmf_OnPk_str(i,j) = Load_net_str(i,j);
            %(Eusable_RE_str=RE gen.+draw from storage-discharge losses)
            Eusable_RE_str(i,j) = Eout_RE(i,j)+H_t(i,j)-ChgDsgLoss(i,j);
                        H_new = H_old - H_t(i,j);
                        %
                        if H_t(i,j)>H_t_max
                           H_t(i,j)=H_t_max;
                         Eout_deficit_str(i,j)=abs(E_ms(i,j))-eff_d*H_t(i,j);
                            Load_net_str(i,j)= Eout_deficit_str(i,j);
                          Eout_dmf_OnPk_str(i,j) = Load_net_str(i,j); %use of
                          %...demand following gen to make up for the deficit
                            ChgDsgLoss(i,j) = (1-eff_d)*H_t(i,j);
                            DsgLoss(i,j) = (1-eff_d)*H_t(i,j);
                    Eusable_RE_str(i,j)=Eout_RE(i,j)+H_t(i,j)-ChgDsgLoss(i,j);
                            H_new = H_old - H_t(i,j);
                        end
                      %
                      elseif H_t(i,j)>StrShare_Pk
                         H_t(i,j) = StrShare_Pk;
                        Load_net_str(i,j) = abs(E_ms(i,j))-eff_d*H_t(i,j);
                         ChgDsgLoss(i,j)=(1-eff_d)*H_t(i,j);
                         DsgLoss(i,j)=(1-eff_d)*H_t(i,j);
                         Eout_deficit_str(i,j) = Load_net_str(i,j);
                         Eout_dmf_OnPk_str(i,j) = Load_net_str(i,j);
```

```matlab
                    Eusable_RE_str(i,j)=Eout_RE(i,j)+H_t(i,j)-ChgDsgLoss(i,j);
                        H_new = H_old - H_t(i,j);
                        %
                        if H_t(i,j)>H_t_max
                            H_t(i,j)=H_t_max;
                            Load_net_str(i,j)=abs(E_ms(i,j))-eff_d*H_t(i,j);
                            Eout_deficit_str(i,j) =  Load_net_str(i,j);
                            ChgDsgLoss(i,j) = (1-eff_d)*H_t(i,j);
                            DsgLoss(i,j) = (1-eff_d)*H_t(i,j);
                            Eout_dmf_OnPk_str(i,j) = Load_net_str(i,j);
                    Eusable_RE_str(i,j)=Eout_RE(i,j)+H_t(i,j)-ChgDsgLoss(i,j);
                            H_new = H_old - H_t(i,j);
                        end
                %
                else   %no discharge/contribution from storage
                end
            %
            else
            end
        %
        end
     H_new =(1-selfdschg)*H_new; %applying self-discharge losses
    %
    h_t(k,1) = H_t(i,j); h_o(k,1) = H_old; h_n(k,1) = H_new;
    l(k,1)=Load(i,j); l_n(k,1)=Load_net(i,j);
    l_n_str(k,1)=Load_net_str(i,j); bse(k,1) = Eout_bse(i,j);
    dmf_OnPk(k,1) = Eout_dmf_OnPk(i,j);
    dmf_OnPk_str(k,1) = Eout_dmf_OnPk_str(i,j);
    dmf_OffPk(k,1) = Eout_dmf_OffPk(i,j);
    dmf_OffPk_str(k,1) = Eout_dmf_OffPk_str(i,j);
    dmf(k,1) = Eout_dmf_OnPk(i,j)+Eout_dmf_OffPk(i,j);
    dmf_str(k,1) = Eout_dmf_OnPk_str(i,j)+Eout_dmf_OffPk_str(i,j);
    s(k,1) = Eout_RE(i,j);   m(k,1) = E_mb(i,j); u(k,1) = E_ms(i,j);
    v(k,1) = Edump_RE(i,j); v_str(k,1) = Edump_RE_str(i,j);
    w(k,1) = Eout_deficit(i,j); w_str(k,1) = Eout_deficit_str(i,j);
    eloss(k,1)=ChgDsgLoss(i,j); soc_hr(k,1) = h_n(k,1)./H_max;
    eREuse(k,1) = Eout_RE(i,j)-Edump_RE(i,j);
    eREuse_str(k,1) = Eusable_RE_str(i,j);
    strshr_pk(k,1) = StrShare_Pk;
    %end
    %
    if j==24
        ChgLevel(i,1)=(H_new/H_max)*100;    %end of day storage energy
capacity
        DailyStrCap(i,1) = H_new;
    end
    %
    StrShare_Pk = 0;
    H_old = H_new;
    %
     end
  end
%
%%%%%%%%%%%%%%%%%%%%%%%%%%%%%%%%%%%%%%%%%%%%%%%%%%%%%%%%%%%%%%%%%%
%OUTPUT
%%%%%%%%%%%%%%%%%%%%%%%%%%%%%%%%%%%%%%%%%%%%%%%%%%%%%%%%%%%%%%%%%%
StrEngCap = max(h_n);    %evaluates max. storage energy capacity
StrPwrCap = max(h_t);    %evaluates max. storage power capacity
StrCapRat = StrEngCap/StrPwrCap;
PkLdRed=(1-(max(dmf)+BaseGen_Annual)/max(l))*100;
```

```matlab
PkLdRed_str=(1-(max(dmf_str)+BaseGen_Annual)/max(l))*100;
%
Total_Load = sum(l); Total_Eout_RE = sum(s);
Total_ChgDsgLoss = sum(eloss); Total_ChgLoss = sum(sum(ChgLoss));
Total_DsgLoss = sum(sum(DsgLoss)); Total_Eout_bse = sum(bse);
Total_Eout_dmf_Offpk = sum(dmf_OffPk);
Total_Eout_dmf_Offpk_str = sum(dmf_OffPk_str);
Total_Eout_dmf_OnPk = sum(dmf_OnPk);
Total_Eout_dmf_OnPk_str = sum(dmf_OnPk_str);
Total_Eout_dmf = sum(dmf); Total_Eout_dmf_str = sum(dmf_str);
Total_Edump_RE = sum(v);
Total_Edump_RE_str = sum(v_str);
Total_Eout_deficit = sum(w);
Total_Eout_deficit_str = sum(w_str);
Total_losses = (Total_Edump_RE/Total_Eout_RE)*100;
Total_losses_str=
((Total_Epv_dump_str+Total_ChgDsgLoss)/Total_Eout_slr)*100;
Total_Eusable_RE = Total_Eout_RE-Total_Edump_RE;    %without storage
Total_Eusable_RE_str1 = sum(eREuse_str);
%
Deficit = (Total_Eout_deficit/Total_Load)*100;
Deficit_str = (Total_Eout_deficit_str/Total_Load)*100;
%
%Average Energy Penetration (based on usable RE output)
Avg_energy_pen = (Total_Eusable_RE/Total_Load)*100;        %
Avg_energy_pen_str = (Total_Eusable_RE_str/Total_Load)*100;
%
Data_out1 = [Avg_energy_pen;PkLdRed;Total_losses;Deficit];
Data_out2 = [Avg_energy_pen_str;PkLdRed_str;Total_losses_str;Deficit_str];
Data_out3 = [l,s,dmf,dmf_str];
Data_out4 = [Data_out1,Data_out2];
%
disp('done !!!')
toc
```

REFERENCES

[1] Akdag, S.A., Dinler, A., "A new method to estimate Weibull parameters for wind energy applications," *Energy Conversion and Management*, 2009, **50**:1761-1766.

[2] U.S. Energy Information Administration (accessed September, 2011) http://www.eia.gov/renewable/annual/preliminary/

[3] U.S regional electricity generation fuel mixes (accessed September, 2011) http://www.nrel.gov/wind/systemsintegration/system_integration_basics.html

[4] Nevada Commission on Economic Development (accessed August, 2011) http://www.diversifynevada.com/industry/renewable_energy/

[5] Sahin, A.Z., "Applicability of Wind-Solar Thermal Hybrid Power Systems in the Northeastern Part of the Arabian Peninsula," *Energy Sources*, 2000, pp. 845-850.

[6] Lew, D., Milligan, M., "How do Wind and Solar Power Affect Grid Operations: The Western Wind and Solar Integration Study," National Renewable Energy Laboratory, 2009.
http://www.nrel.gov/wind/systemsintegration/wwsis.html

[7] Parsons, B., et al., "Impacts of large amounts of wind power design and operation of power systems; results of IEA collaboration," *AWEA Windpower 2008*, Houston, TX, 2008.

[8] Hoste, G.R.G, Dvorak, M.J., Jacobson, M.Z., "Matching hourly and peak demand combining different renewable energy sources: a case study for California in 2020."
http://www.stanford.edu/group/efmh/jacobson/Articles/I/HosteFinalDraft.pdf

[9] Denholm, P., Margolis, R.M., 2007, "Evaluating the limits of solar photovoltaics (PV) in electric systems utilizing energy storage and other enabling technologies," *Energy Policy*, **35**:4424-4433.

[10] Vanek, F.M. and Albright, L.D., "Energy systems engineering: evaluation & implementation," McGraw-Hill, New York, 2008 (225).

[11] American Wind Energy Association, "U.S. wind industry annual market report year ending 2010," 2011.
http://www.awea.org/_cs_upload/events/7302_1.pdf

[12] Zahedi, A., "Maximizing solar PV penetration using energy storage technology," *Renewable and sustainable energy reviews*, 2011, **15(1)**: 866-870.

[13] Beaudin, M., et al, "Energy storage for mitigating the variability of renewable electricity sources: An updated review*" Energy for Sustainability Development*, 2010, **14**:302-314.

[14] Gardner, J., Haynes, T., 2007, Overview of compressed air energy storage, Sustainabilty Research, Boise State University, ER-07-001. (accessed on 08/01/2011) http://coen.boisestate.edu/WindEnergy/resources/ER-07-001.pdf

[15] Ibrahim, H., Ilinca, A., Perron, J., "Energy storage systems – characteristics and comparisons," *Renewable & Sustainability Energy Reviews*, 2008, **12**:1221-1250.

[16] Hadjipaschalis I, Poullikkas A, Efthimiou V., "Overview of current and future energy storage technologies for electric power applications," *Renewable Sustainable Energy Reviews*, 2009, **13(6–7)**:1513–1522.

[17] Solomon, A.A., Faiman, D., Meron, G., "Properties and uses of storage for enhancing the grid penetration of very large photovoltaic systems," *Energy Policy*, 2010, **38**:5208-5222.

[18] Chen H, Cong Y, Yang W, Tan C, Li Y, Ding Y., "Progress in electrical energy storage system: a critical review," *Prog. Nat. Sci*., 2009, **19(3)**:291–312.

[19] Schaber, C., et al., "Utility-scale storage of renewable energy," *The Electricity Journal*, doi:10.1016/j.tej.2004.05.005, 2004,

[20] U.S. Department of Energy Report, "20% wind energy by 2030: increasing wind energy's contribution to U.S. electricity supply," 2008. http://wpadev.nrel.gov/pdfs/20_percent_wind_2.pdf

[21] Parsons, B., et al., "Grid impacts of wind power: a summary of recent studies in the United States," *Wind Energy*, 2004, **7**:87–108.

[22] Weisser, D., Garcia, R.S., "Instantaneous wind energy penetration in isolated electricity grids: concepts and review," *Renewable Energy*, 2005, **30**:1299–1308.

[23] Milborrow D., "Penalties for intermittent sources of energy," Working paper for the UK PIU energy review," Cabinet Office, London, 2001.

[24] Stodola, N., and Modi, V., "Penetration of solar power without storage," *Energy Policy*, 2009, **37**:4730-4736.

[25] Denholm, P., Margolis, R.M., "Evaluating the limits of solar photovoltaics (PV) in traditional electric power systems," *Energy Policy*, 2007, **35**:2852-2861.

[26] Solomon, A.A., Faiman, D., Meron, G., "Grid matching of large-scale wind energy conversion systems, alone and in tandem with large-scale photovoltaic systems: An Israeli case study," *Energy Policy*, 2010, **38**:7070-7081.

[27] Heide, D, et al., "Seasonal optimal mix of wind and solar power in a future, highly renewable Europe," *Renewable Energy*, 2010, **35**:2483-2489.

[28] Chowdhury, B.H., "Central station photovoltaic plant with energy storage for utility peak load leveling," IEEE, 899041, 1989.

[29] National Renewable Energy Laboratory (NREL), Solar Advisor Model (2010) https://www.nrel.gov/analysis/sam/

[30] NREL/3TIER Western Wind and Solar Integration Study http://wind.nrel.gov/

[31] Mowers, M. et al., "Correlation between geographically dispersed concentrating solar power and demand in the United States," *Proceedings of ASME 2010 4th International Conference on Energy Sustainability,* Phoenix, AZ, 2010.

[32] Solomon, A.A., Faiman, D., Meron, G., "An energy-based evaluation of the matching possibilities of a very large photovoltaic plants to the electricity grid: Israel as a case study ," *Energy Policy*, 2010, **38:**5457-5468.

[33] Wikipedia, Hybrid power systems (accessed September 4, 2011)

[34] Agyenim-Boateng, K. and Boehm, R.F., "Impact of storage integrated solar photovoltaic (PV) power system on utility peak loads," *Proceedings of ASME 2011 5th International Conference on Energy Sustainability,* Washington, DC, 2011.

VITA

Graduate College
University of Nevada, Las Vegas

Kwame Agyenim-Boateng

Local Address:
　1455 E. Rochelle Avenue
　Unit 27
　Las Vegas, NV 89119

Degrees:
　Bachelor of Science in Mechanical Engineering, 2002

　Kwame Nkrumah University of Science and Technology, Kumasi, Ghana

　Master of Science in Renewable Energy Systems Technology, 2006

　Loughborough University, Loughborough, Britain

Publications:
　Agyenim-Boateng, K. and Boehm, R.F., "Impact of Storage Integrated Solar
　Photovoltaic (PV) Power System on Utility Peak Loads," *Proceedings of ASME 2011
　5th International Conference on Energy Sustainability,* Washington, DC, 2011.

　Sahm, A., Agyenim-Boateng, K., Hynes, K., Hammer, K., Roberts, T., Boehm, R.F.,
　Stone, K., "Two Types of Calorimeters for Assessing Fresnel Lens Performance in
　Concentrating Solar Systems Measuring Solar Flux," *Proceedings of ASME 2011 5th
　International Conference on Energy Sustainability,* Washington, DC, 2011.

Thesis Title: Energy-Based Analysis of Utility Scale Hybrid Power Systems

Thesis Examination Committee:

Committee Chair, Dr. Robert F. Boehm, PhD

Committee Member, Dr. Yitung Chen, PhD

Committee Member, Dr. Suresh B. Sadineni, PhD

Graduate College Representative, Dr. Yahia Baghzouz, PhD